Uncovering the Interleukin-12 Pharmacokinetic Desensitization Mechanism and Its Consequences with Mathematical Modeling

Jonathon DeBonis[a], Omid Veiseh[a], and Oleg A. Igoshin[a,b]

[a]Department of Bioengineering, Rice University, Houston, Texas, USA.

[b]Center for Theoretical Biological Physics, Department of Chemistry, Department of Biosciences, Rice University, Houston, Texas, USA

Corresponding Author: Oleg Igoshin, igoshin@rice.edu, Department of Bioengineering, Rice University, Houston, Texas, USA.

Acknowledgments

An early version of this work was presented as a late-breaking abstract at the BMES 2023 Annual Meeting.

This work was partly supported by the Welch Foundation (grant C-1995 to O.A.I.) and by the Advanced Research Projects Agency for Health (ARPA-H) under Award Number AY1AX000003. The simulations were performed on the Rice University's Center for Research Computing equipment acquired with the Big-Data Private-Cloud Research Cyberinfrastructure MRI-award funded by the NSF under grant CNS-1338099. The content is solely the responsibility of the authors and does not necessarily represent the official views of the Welch Foundation, the Advanced Research Projects Agency for Health, or the NSF.

Conflicts of Interest

O.V. holds equity and O.A.I has consultant position in Avenge Bio. The authors declare that they have no other competing interests.

Keywords: interleukin-12, pharmacokinetics, mathematical modeling, cancer immunotherapy, drug transport, dynamical systems analysis

Abstract

The cytokine interleukin-12 (IL-12) is a potential immunotherapy because of its ability to induce a Th1 immune response. However, success in the clinic has been limited due to a phenomenon called IL-12 desensitization – the trend where repeated exposure to IL-12 leads to reduced IL-12 concentrations (pharmacokinetics) and biological effects (pharmacodynamics). Here, we investigated IL-12 pharmacokinetic desensitization via a modeling approach to (i) validate proposed mechanisms in literature and (ii) develop a mathematical model capable of predicting IL-12 pharmacokinetic desensitization. Two potential causes of IL-12 pharmacokinetic desensitization were identified: increased clearance or reduced bioavailability of IL-12 following repeated doses. Increased IL-12 clearance was previously proposed to occur due to the upregulation of IL-12 receptor on T-cells that causes increased receptor-mediated clearance in the serum. However, our model with this mechanism, the accelerated-clearance model, failed to capture trends in clinical trial data. Alternatively, our novel reduced-bioavailability model assumed that upregulation of IL-12 receptor on T-cells in the lymphatic system leads to IL-12 sequestration, inhibiting the transport to the blood. This model accurately fits IL-12 pharmacokinetic data from three clinical trials, supporting its biological relevance. Using this model, we analyzed the model parameter space to illustrate that IL-12 desensitization occurs over a robust range of parameter values and to identify the conditions required for desensitization. We next simulated local, continuous IL-12 delivery and identified several methods to mitigate systemic IL-12 exposure. Ultimately, our results provide quantitative validation of our proposed mechanism and allow for accurate prediction of IL-12 PK over repeated doses.

Introduction

Inteleukin-12 (IL-12) is a heterodimeric cytokine consisting of the p35 α subunit and the p40 β subunit[1]. The unmodified form of IL-12 has a molecular weight of 58.9 kDa; however, its glycosylated form migrates as a 65-75 kDa protein in SDS PAGE[2]. The average value for the molecular weight of 70 kDa is usually reported and therefore the heterodimer form is referred to as IL-12 p70[1,3]. IL-12's immunological activity is characterized by causing differentiation of CD4+ helper T-cells (Th-cells) into the Th1 phenotype, leading to the production of pro-inflammatory cytokines and immune system activation[4]. The primary cytokine induced by IL-12 activity is IFNγ, but TNFα, GM-CSF, IL-2, and IL-8 are also known to be produced in response to IL-12 stimulus[1,5]. Immune activation is achieved through the binding of IL-12 to its receptor, which ultimately leads to the activation of STAT4[1,5,6]. IL-12's ability to trigger robust immune system activation motivates its investigation as a potential cancer immunotherapy.

The first clinical trial investigating IL-12 was initiated in 1997 for the treatment of cancer patients with advanced malignancies[1,7]. Here, patients were first treated with an i.v. test dose of IL-12 two weeks before receiving five times weekly i.v. doses of IL-12 every 28 days[7]. A phase two trial was initiated shortly after following the same dose regimen without the test dose. In stark contrast to the phase one trial, this trial was quickly terminated after severe toxicities, including treatment-related patient deaths[8]. It was apparent that prior exposure to IL-12 desensitizes patients to IL-12's immunological activity, evident through the ~5-fold increase in measured serum IFNγ in patients treated with the same dose in the PII trial.

IL-12 desensitization has been observed in a large number of additional clinical trials, with results illustrating that both IL-12 pharmacokinetics (PK) and pharmacodynamics (PD) are desensitized[9–18]. PD desensitization is characterized by reduced IFNγ levels following repeated doses[7,8,14,17],

whereas PK desensitization causes reduced IL-12 concentrations.[15,16,19]. Furthermore, PK and PD desensitization appear to be caused by separate mechanisms due to a difference in the timescale in which these phenomena occur. In a study of repeated subcutaneous IL-12 doses in mice, measured serum IL-12 concentrations decreased with every dose administered, whereas measured serum IFNγ concentrations decreased after three doses were administered[19]. Despite increasing tolerance to IL-12 administration, studies have shown that response to IL-12 treatment is also hindered by desensitization[12,14,20]. Ultimately, due to its implications in both tolerability and response to IL-12 treatment, understanding the mechanism causing PK and PD desensitization is essential for the optimization of IL-12 therapies.

Several mechanisms have been proposed in the literature to explain IL-12 PK and PD desensitization; however, none have been validated quantitatively. Importantly, results from clinical trials illustrate that anti-drug antibodies (ADAs) are rarely formed against IL-12[7,11,15,19], suggesting a different mechanism for desensitization. In terms of PK desensitization, the primary molecular mechanisms discussed revolve around the upregulation of IL-12 receptors on T-cells following IL-12 stimulation[15,21]. Increased expression of IL-12 receptor leads to higher levels of receptor-mediated clearance, which can lead to faster serum clearance or higher levels of IL-12 sequestration during transport into the blood. Overall, this would lead to reduced serum IL-12 concentrations due to increased clearance or lower bioavailability, and these effects are apparent almost immediately after repeated doses. Conversely, desensitization of IL-12's immunological effects is delayed and tends to occur after several doses have been administered[15]. Discussed mechanisms for this effect include downregulation of STAT4 after sustained IL-12 signaling[22] and adaptive T-cell exhaustion due to IL-12 stimulation[10,18].

The absorption, distribution, metabolism, and elimination (ADME) properties of IL-12 are not characterized in detail, but the large molecular weight of IL-12 (70 kDa) provides insight into its absorption and elimination characteristics. As molecules with greater molecular weights than 16 kDa are absorbed into the blood primarily by the lymphatic system[23], it follows that IL-12 likely is absorbed via the same route following administration into peripheral tissues. Similarly, molecules with molecular weights greater than 50 kDa are typically eliminated via intracellular lysosomal proteolytic degradation rather than renal clearance due to the relatively small glomeruli pore size[24,25]. However, renal clearance may still influence IL-12 elimination[26].

Here, focusing on PK desensitization, we investigated proposed mechanisms for IL-12 PK desensitization in literature via a modeling approach. More specifically, we developed mathematical models containing two different mechanisms of interest for IL-12 PK desensitization and challenged these models to fit clinical trial data. Furthermore, after identifying the mechanism that is consistent with the data, we determine the parameter regime under which significant desensitization can occur and use the model with our proposed mechanism to identify potential strategies for mitigating systemic toxicity to IL-12 treatment.

Methods

Clinical Trial Data Collection

Three clinical trials with IL-12 PK measurements over multiple subcutaneous doses of IL-12 were identified[15–17,19]. **Table 1** contains information regarding the dosing regimens investigated, the patient populations, and the doses where PK measurements were taken. These three clinical trials were determined to be well suited for this investigation because they provide IL-12 PK data after repeated doses of IL-12 with either different dosing regimens or doses selected for PK analysis

(**Figure 1A**). Two of the clinical trials investigated report IL-12 time-course measurements, whereas the other trial only reports PK metrics, including area under the curve (AUC), maximum concentration (C_{max}), and time of maximum concentration (t_{max}). In trials with time-course data, the numerical values were extracted from figures using GraphGrabber2.0.2 (Quintessa).

Table 1: Information on clinical trials analyzed in this investigation.

Clinical Trial	**Dose Amounts and Regimen**	**Number of Patients**	**Patient Indications**	**Sampling Times**
Phase I trial of Subcutaneous Recombinant Human Interleukin-12 in Patients with Advanced Renal Cell Carcinoma[15]	0.1 – 1.5 µg/kg on days 1, 8, and 15 in a 28-day cycle.	51	Advanced renal cell carcinoma. 42 patients received prior therapy.	Baseline and 10, 24, 48, 72, 96, and 168 h post dose on doses 1 or 3 in cycle 2.
Phase I Study of Subcutaneously Administered Recombinant Human Interleukin 12 in Patients with Advanced Renal Cell Cancer[16]	0.5, 1.0, 1.25 µg/kg three times weekly for two weeks following a test dose one week prior.	28	Advanced renal cell carcinoma. 26 patients received prior therapy.	Baseline and 4, 6, 8, 10, 12, 18, 24, 30 , 26, 48, 72, 96 h after test dose and 4, 6, 8, 10, 12, 18, 24, and 36 h after repeat doses.
Down-regulation of the pharmacokinetic-pharmacodynamic response to interleukin-12 during long-term administration to patients with renal cell carcinoma and evaluation of the mechanism of this "adaptive response" in mice[19]	0.1, 0.5, 1.0 µg/kg on days 1, 8, and 15 of a 28-day cycle.	24	Advanced or metastatic renal cell carcinoma. 15 patients received prior therapy.	Baseline and 2, 4, 8, 8, 10, 16, 24, 30, 34, 48 h post dose on dose 1 of cycle 1 and dose 3 of cycle 2.

Mathematical Models of IL-12 PK and Numerical Simulation

Mathematical models utilized in this investigation were constructed as a system of ordinary differential equations governing IL-12 dosing, transport, target binding and upregulation, and clearance. The notation and the meaning for each model parameter are found in **Table 2.** Below, we explain the model equations in simple terms; detailed derivations for these equations are provided in the supplementary text.

Simulation of bolus IL-12 injection is represented by setting the initial concentration of IL-12 in the dosing compartment *i,* $IL12_{i,0}$, computed based on the dose amount and the volume of the compartment:

$$IL12_{i,0} = \frac{D}{V_i} \tag{1}$$

Once in the dosing compartment, IL-12 either leaves the compartment via lymphatic transport or degradation. The concentration of IL-12 in the dosing compartment is therefore described by:

$$\frac{dIL12_i}{dt} = -J_{ki}\, IL12_i - k_{DG} IL12_i \tag{2}$$

The first term accounts for IL-12 transport, which is modeled as unidirectional transport mediated by lymph fluid flow[23] and represented as a first-order process. The second term describes the first-order degradation rate in the subcutaneous space with the rate determined by the absolute bioavailability, F, as follows:

$$k_{DG} = \frac{1-F}{F} J_{ki} \tag{3}$$

This relationship is derived such that a bioavailability of 100% leads to a degradation rate constant of zero. After leaving the dosing compartment, IL-12 either enters intermediate compartment *k* then enters the blood or enters the blood directly. In the former case, the concentration of IL-12 in compartment *k* is described by the following equation:

$$\frac{dIL12_k}{dt} = \frac{V_i}{V_k} J_{ki}\, IL12_i - J_{Bk} IL12_k \tag{4}$$

The flux of IL-12 into the intermediate compartment is represented by the first term, which is equal to the total flux of IL-12 out of the dosing compartment scaled by the ratio of the compartment volumes. The second term represents IL-12 transport from the intermediate

compartment to the blood compartment. Similarly, the concentration of IL-12 in the blood (denoted by subscript B) compartment is described as follows:

$$\frac{dIL12_B}{dt} = \frac{V_k}{V_B} J_{Bk} IL12_k - k_{CB} IL12_B \tag{5}$$

As in equation 4, the first term here represents IL-12 flux into the blood. In absence of receptor binding, IL-12 is cleared from the blood according to the second term which represents general systemic clearance likely mediated through proteolytic degradation[24,25]. In the case where IL-12 enters the blood directly rather than through an intermediate compartment, V_k, J_{Bk}, and $IL12_k$ in equation 5 are replaced by V_i, J_{Bi}, and $IL12_i$, respectively.

In model compartments in which receptor binding and STAT4 activation occur, the concentration of IL-12:receptor complex is described as follows:

$$\frac{dC_x}{dt} = k_{on}\, IL12_x\, R_x - k_{int} C_x \tag{6}$$

The first term represents the rate of IL-12:receptor binding, which we assume to be irreversible for simplicity, and the second term describes the first-order internalization of the complex. Formation of complex leads to STAT4 activation that is modeled by the following expression that assumes non-cooperative binding and a quasi-steady state:

$$pSTAT_x = \frac{\widetilde{C_x}}{\widetilde{C_x} + IC_{pSTAT}} \tag{7}$$

In this equation, we use the number of complexes per cell ($\widetilde{C_x}$) because our model predicts the total concentration of complexes in all the cells of the compartment, but STAT4 is activated on a single cell basis. To predict the level of STAT4 activation in each cell, $\widetilde{C_x}$ is calculated by assuming homogenous distribution of complex across the population of cells in the compartment according to the following:

$$\widetilde{C_x} = A\frac{C_x V_x}{N_x}, \tag{8}$$

This equation converts the concentration of receptors in the compartment (pmol mL^{-1}) to the number of complexes per T-cell (# cells^{-1}) using Avogadro's number ($A = 6e12\frac{\#}{\text{pmol}} = 6e23\frac{\#}{\text{mol}}/1e12\frac{\text{pmol}}{\text{mol}}$), the volume of the compartment, and the number of T-cells in the compartment. In our models, activation of STAT4 leads to upregulation of IL-12 receptor on T-cells. Accordingly, the concentration of IL-12 receptor in compartments is represented by:

$$\frac{dR_x}{dt} = \frac{N_x}{V_x}k_R + \frac{N_x}{V_x}\alpha\, pSTAT_x - k_{on}IL12_x R_x - k_{CR}R_x \tag{9}$$

The first two terms in this ordinary differential equation represent basal and upregulated IL-12 receptor expression, respectively. The production rates, k_R and α, are given in units of pmol cells^{-1}; thus, we scale by the number of cells divided by the volume to convert to pmol mL^{-1} days^{-1}. The third term here represents consumption of IL-12 receptor due to binding, and the last term represents unbound internalization of IL-12 receptor.

The initial concentration of receptor in compartment x, $R_{SS.x}$ (pmol mL^{-1}), can be set based on R_0, the basal amount of IL-12 receptor on the surface of T-cells (pmol), as follows:

$$R_{SS,x} = \frac{R_0 N_x}{V_x} \tag{10}$$

To ensure that this value is consistent with our model in the absence of IL-12, we constrain the basal production rate according to:

$$k_R = R_0 k_{CR} \tag{11}$$

All models in this investigation were constructed using this framework, differing in the compartment in which receptor binding takes place. Models were simulated in MATLAB

(R2020b) using the ODE solver ode15s. All option arguments are set to default except for the non-negative argument set to one and the absolute tolerance set to 1e-12.

Table 2: General model parameters, species, meanings.

Species	**Meaning (Units)**
$IL12_x$	Concentration of IL-12 in compartment *x* (pmol mL^{-1}).
R_x	Concentration of IL-12 receptor in compartment *x* (pmol mL^{-1})
C_x	Concentration of IL-12:IL-12 receptor in compartment *x* (pmol mL^{-1}).
$\widetilde{C_x}$	Number of IL-12:IL-12 receptor complexes per T-cell in compartment *x* (# cells^{-1})
$pSTAT_x$	Fractional of maximum STAT4 activation on T-cells (unitless)
Parameter	**Meaning (Units)**
D	IL-12 dose administered (pmol).
J_{xy}	Normalized lymphatic fluid flow rate from compartment *y* to compartment *x* (days^{-1}).
k_{DG}	First order IL-12 degradation rate constant in the dosing compartment (days^{-1})
F	Absolute IL-12 bioavailability defined as fraction of IL-12 leaving the dosing compartment instead of being degraded (unitless)
k_{CB}	First order IL-12 systemic clearance rate constant from blood compartment (days^{-1})
k_{on}	IL-12:IL-12 receptor association rate constant (mL pmol^{-1} days^{-1})
k_{int}	IL-12 receptor bound internalization rate constant (days^{-1})
k_{CR}	IL-12 receptor unbound internalization rate constant (days^{-1})
IC_{pSTAT}	Number of IL-12:IL-12 receptor complexes per T-cell required for half-maximum STAT4 activation (# cells^{-1})
k_R	Basal IL-12 receptor production rate per T-cell (pmol cells^{-1} days^{-1})
α	Receptor upregulation feedback coefficient (pmol cells^{-1} days^{-1})
N_x	Number of T-cells in compartment *x* (#)
R_0	Basal amount of IL-12 receptor on T-cell (pmol cells^{-1})

V_x	Volume of compartment x (mL)

Data Fitting and Parameter Estimation Procedures

We utilized two methods to fit our model to clinical trial data. Global optimization was implemented using MATLAB's particleswarm algorithm, and ensemble local optimization was implemented by randomly sampling parameter sets within optimization boundaries and locally optimizing using MATLAB's patternsearch algorithm[27]. The fitness functions used for optimization varied based on the type of PK data presented; for specific details, see the supplementary text.

Results

Two alternative models of desensitization describing literature-proposed mechanisms were developed.

We first identified proposed mechanisms for IL-12 PK desensitization in literature as a basis for developing our mathematical models. Analysis of preclinical and clinical trials of IL-12 provided evidence for two distinct causes of IL-12 PK desensitization: increased clearance or decreased bioavailability following repeated doses[11,15,16,19]. While both were proposed in the literature, neither cause has been validated quantitatively. Thus, we aimed to formulate molecular mechanisms for the identified causes of IL-12 desensitization in literature and validate whether these mechanisms can account for trends in clinical trial data.

Two models were constructed containing molecular mechanisms for increased clearance or reduced bioavailability after repeated IL-12 doses, respectively. Both models contain equations representing IL-12 dosing, transport, and degradation in the subcutaneous space. Furthermore, IL-12 binding to IL-12 receptors on T-cells also occurs in both models. Formation of IL-12:IL-12

177 receptor complex activates STAT4 based on a quasi-steady state assumption, and STAT4 activation

178 upregulates the production of IL-12 receptor[16,19,21].

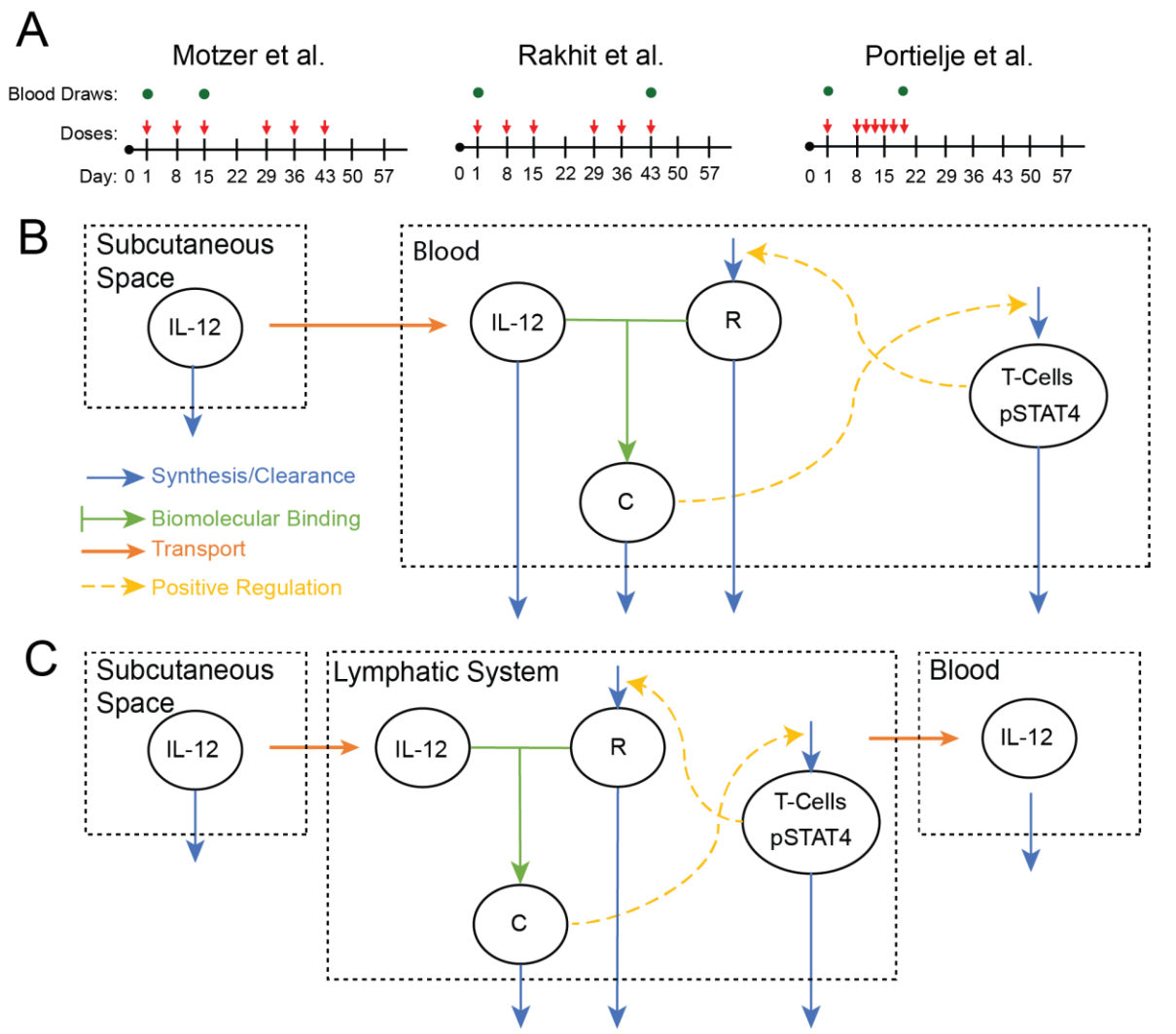

Figure 1: Clinical trial dosing information and schematics of models used in this investigation. A) Timelines illustrating dose regimens and doses where blood measurements are taken in three clinical trials used in this investigation. B) Schematic of accelerated-clearance model. C) Schematic of reduced-bioavailability model.

179 The main difference between the two models is the compartment where receptor binding and

180 upregulation occur. Our first model was designed such that upregulation of the IL-12 receptor on

181 T-cells leads to accelerated clearance of IL-12 from the serum. Accordingly, IL-12 binds its

receptor in the blood compartment such that clearance occurs from receptor binding and standard first-order clearance/degradation. As no significant interactions occur in the lymphatic system based on this mechanism, the lymphatic system compartment is omitted from this model. Conversely, our second model was designed such that receptor upregulation leads to reduced bioavailability. In this case, receptor binding and upregulation occur in the lymphatic system compartment during transport into the blood; therefore, upregulation of the receptor leads to IL-12 sequestration in the lymphatic system. Overall, both models are based on the principle that STAT4 activation in T-cells leads to upregulated IL-12 receptor expression, with the key difference being whether this leads to accelerated clearance or reduced bioavailability. As such, we correspondingly term our models as the accelerated-clearance model (**Equations S1-S9, Figure 1B**) and the reduced-bioavailability model (**Equations S10-S19, Figure 1C**).

The accelerated-clearance model fails to accurately predict IL-12 PK following repeated doses.

To understand if the accelerated-clearance model can capture trends of IL-12 desensitization in published clinical trial data, we fitted the model to three separate clinical PK datasets of repeated subcutaneous IL-12 injections with global optimization. The results are presented in **Figures 2A-B** (see also: **SI Text, Supplementary Tables S1-2**) and demonstrate that this model captures the relative magnitude of IL-12 desensitization, but the overall shape of time-course curves is inaccurate. More specifically, the data from clinical trials suggests that neither maximal time nor half-life changes significantly with repeated exposure to IL-12[15,16]. Accelerated-clearance with repeated doses would lead to changes in both of these PK metrics, causing this model to be incapable of accurately predicting IL-12 PK. Therefore, we conclude that IL-12 PK desensitization is unlikely to directly result from IL-12 upregulation in the blood. Accordingly,

the proposed mechanism in the accelerated-clearance model alone cannot account for IL-12 PK desensitization.

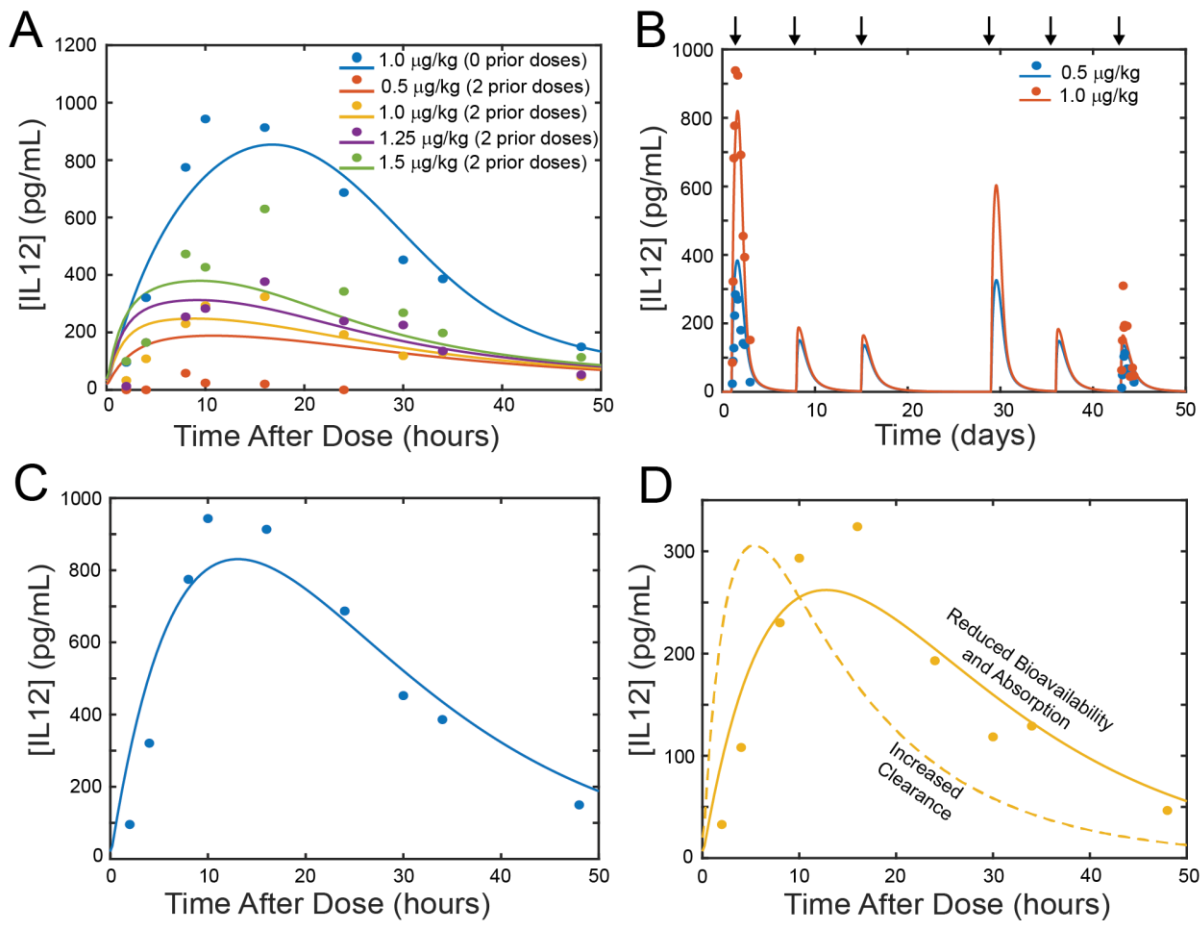

Figure 2: Accelerated-clearance model fitness to clinical trial data with and without feedback. A) Accelerated-clearance model fit to clinical trial data presented by Motzer et al. B) Accelerated-clearance model fit to clinical trial data presented by Rakhit et al. Black arrows represent dose administration C) Accelerated-clearance model fit to IL-12 time course data following 1.0 μg/kg administration with no prior doses from Motzer et al. D) Accelerated-clearance model refit to IL-12 time course data 1.0 μg/kg administration with two prior doses from Motzer et al. All model parameters other than bioavailability and absorption (solid line) or systemic clearance rate (dashed line) fixed to values in C).

To determine the shifts in the model parameter space associated with desensitization, we next analyzed the accelerated-clearance model without feedback. To do this, we removed feedback

from the accelerated-clearance model by setting the feedback parameter α equal to zero (see supplementary equation S3), and separately fit IL-12 PK data from patients with and without prior IL-12 exposure. The data presented by Motzer and colleagues contains IL-12 serum concentrations at various time points after 1.0 μg/kg doses with and without prior exposure to IL-12. To determine the shifts in the PK parameter associated with prior exposure to IL-12, we first fit the dataset without prior exposure to estimate the model parameters in the absence of desensitization (**Figure 2C**). Leaving all other parameters fixed, we then fit the dataset with previous exposure only varying either the IL-12 clearance rate (k_{CB}) or IL-12 bioavailability and absorption (J_{BS} and F). Manipulating IL-12 clearance did not allow for the desensitized dataset to be captured with high fitness but altering bioavailability and absorption accurately fit both the magnitude of desensitization and the shape of the data (**Figure 2D**). Ultimately, these results suggested that a mechanism related to the bioavailability and absorption of IL-12 in the blood is more likely to contribute to IL-12 PK desensitization.

The reduced-bioavailability model accurately predicts IL-12 PK across all three clinical trials.

Next, we sought to determine whether our proposed mechanism influencing IL-12 bioavailability and transport into the blood can accurately fit IL-12 PK data reported in clinical trials. To this end, we fit the reduced-bioavailability model to all three clinical trials via global optimization. Optimization results illustrate that this model can fit these datasets accurately (**Figures 3A-B, SI Text, Supplementary Tables S3-4**). Importantly, unlike the accelerated-clearance model, this model captures both the magnitude and overall shape of the datasets for all doses except the 0.5 μg/kg level in the dataset presented by Motzer and colleagues[15]. There is nonlinearity in the dataset that leads to concentrations at this dose level to be overpredicted. We suspect that this is due to the presence of target mediated drug disposition (TMDD)[28], which is not currently included in our

model. Indeed, if we add target binding and dynamics into the blood compartment of the reduced-bioavailability model this nonlinearity is able to be captured (**SI Text, Supplementary Figure S1**). As our model is still able to predict the PK at larger doses accurately, we continued our analyses with the unmodified reduced-bioavailability model. Overall, the ability of the reduced-bioavailability model to fit all three datasets with different dose regiments supports its robustness.

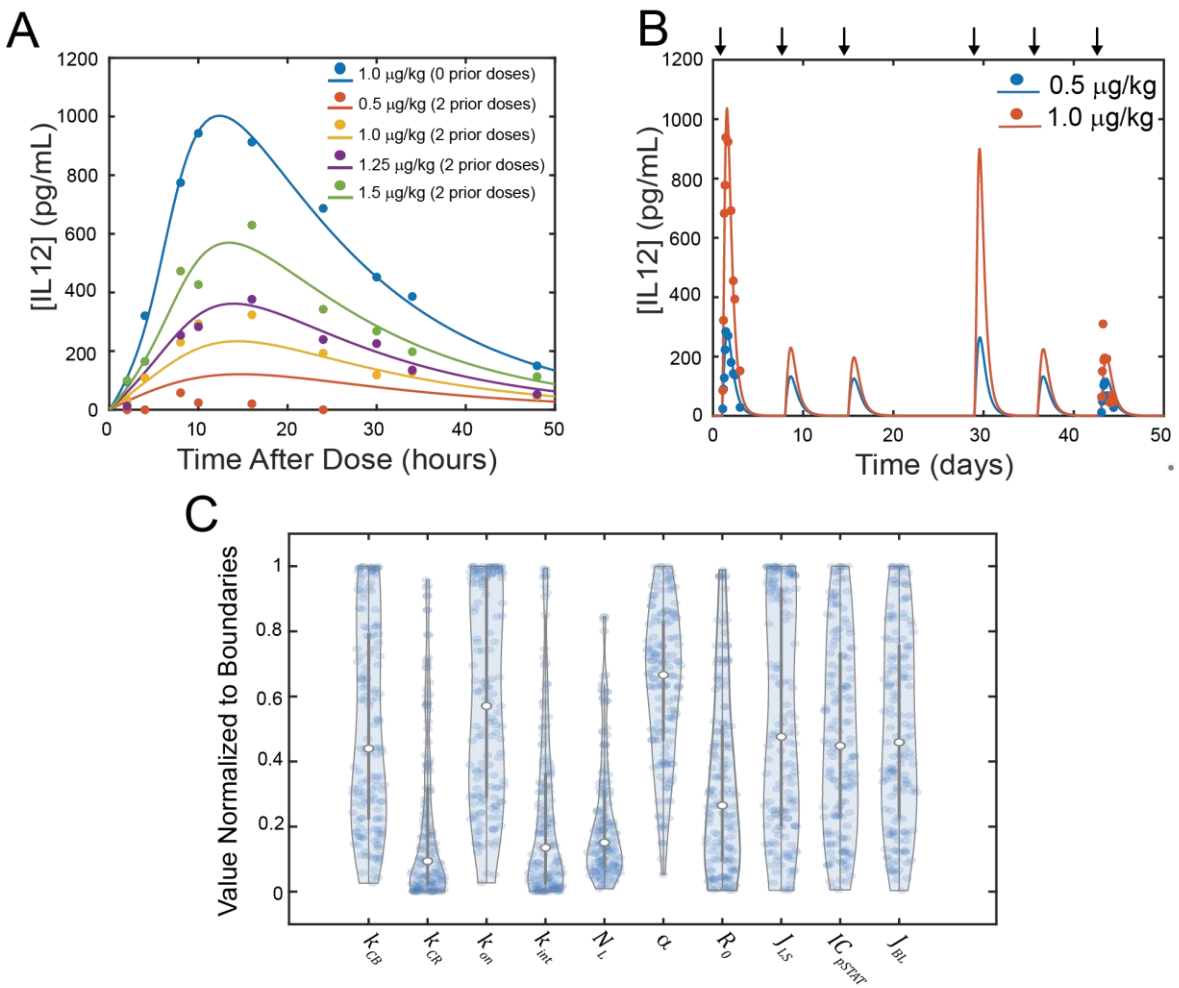

Figure 3: Reduced-bioavailability model fit to clinical trial data. A) Reduced-bioavailability model fit to clinical trial data presented by Motzer et al. after global optimization. B) Reduced-bioavailability model fit to clinical trial data presented by Rakhit et al. after global optimization. C) Distribution of generated ensemble fit to all three clinical trials following local optimization of randomly sampled parameter sets within boundaries (50 parameter sets per clinical trial).

236 As PK parameters often vary between patients[29], we sought to determine if our model can
237 accurately fit IL-12 PK data over a wide range of biologically relevant parameter values. An
238 ensemble of parameter sets was obtained by locally optimizing many sampled parameter sets to
239 each clinical trial. This method yields model parameter sets with slightly worse fitness to data
240 when compared to global optimization (**SI Text, Supplementary Figure S2**) but gives us a
241 distribution of parameter sets to analyze. Analysis of parameter distributions from all three fits
242 illustrates that model parameters are not tightly constrained and are widely distributed over the
243 optimization boundaries (**Figure 3C**). Furthermore, the distribution of parameter values does not
244 vary significantly based on the clinical trial used for fitting (**SI text, Supplementary Figure S3).**
245 These results illustrate that the prediction of IL-12 PK desensitization occurs over a large range of
246 parameter values and that the available data does not sufficiently restrict the PK parameters.

247 *Analysis of model behavior illustrates the effects of dosing regimen and model parameters on*
248 *desensitization.*

249 To gain insight into how the dosing regimen and model parameters influence the amount of IL-12
250 PK desensitization in the reduced-bioavailability model, we simulated the reduced-bioavailability
251 model under various dosing conditions and parameter values to determine the effects on the
252 amount of desensitization predicted. For this analysis we use the parameters obtained via global
253 optimization to the data presented by Motzer and colleagues[15]. We first investigated the amount
254 of desensitization our model predicts following two consecutive doses of IL-12 with varying dose
255 amounts (**Figure 4A**) and time between doses (**Figure 4B**). Predictions illustrate that the extent
256 of desensitization increases with higher doses and doses that are closer in time. We hypothesized
257 that desensitization is mainly controlled by the concentration of receptor remaining in the
258 lymphatic system by the time of the next dose. A larger dose leads to increased STAT4 activation

and a more significant increase in receptor expression, and doses closer in proximity lead to less receptor clearance back to baseline before the next dose. To expand on this hypothesis, we generated an ensemble of 10,000 parameter sets varying $k_{CR}, k_{int}, N_{cells}, \alpha, R_0$, and IC_{pSTAT} between 50% and 150% of the optimized values holding all other parameters constant and simulated consecutive s.c. doses of IL-12 one week apart. Analysis of the ensemble simulation results validated our hypothesis that the extent of desensitization predicted correlates with the difference in receptor concentrations between the first and second dose (**SI Text, Supplementary Figure S7**).

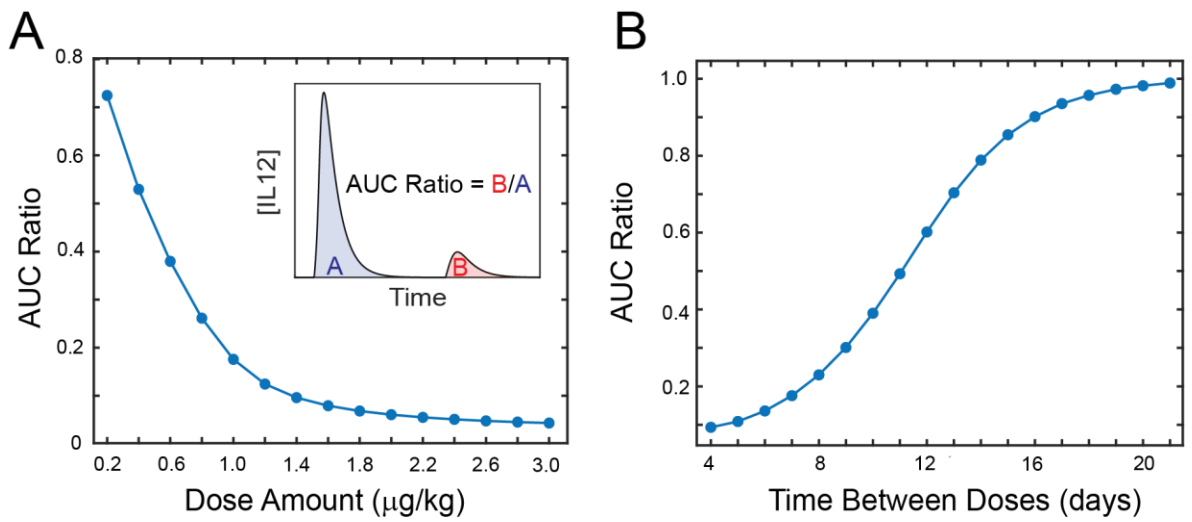

Figure 4: Analysis of model and dosing parameters influence on predicted amounts of desensitization. A) Predicted amount of desensitization after two consecutive IL-12 doses seven days apart at varying dose levels. Inset: visual representation of AUC ratio. B) Predicted amount of desensitization after two consecutive 1.0 μg/kg doses with varying time between doses.

We next analyzed how variations in specific parameters related to receptor upregulation influence the amount of desensitization predicted. First, local sensitivity analyses were implemented for two and three consecutive doses of 0.5, 1.0, and 1.5 μg/kg, revealing which model parameters were most sensitive to the predicted amount of desensitization (**SI Text, Supplementary Figure S3**). The only model parameter with negligible impact on desensitization was k_{CB}, the clearance rate

of IL-12 from the blood. All other parameters had log gain sensitivities that were close to one in some doses simulated. Of interest, parameters related to the amount of receptor initially (R_0, N_{cells}) and the lifetime of receptor (k_{CR}, k_{int}) had log gain sensitivities greater than one at some dose levels.

Simulation of local IL-12 delivery reveals potential strategies for limiting systemic exposure to IL-12 while maintaining desired local concentrations.

Next, we sought to explore the consequences of our proposed mechanism in designing IL-12 therapies for limiting systemic exposure to IL-12. As current interest in IL-12 therapy revolves around local cytokine delivery via cell or gene therapy, we modified the reduced-bioavailability model to represent bolus or continuous delivery of IL-12 to the peritoneal cavity (**SI Text, Supplementary Figure S5**). This model is structurally identical to the reduced-bioavailability model, except the volume of the dosing compartment is increased to the volume of the peritoneal cavity, the transport parameters are re-estimated, and a 0th order intraperitoneal IL-12 production term is introduced for simulation of continuous delivery. We selected intraperitoneal administration for these analyses because it is a common site of administration for IL-12-based therapies[30–32], and a PK dataset was available reporting both intraperitoneal and serum IL-12 concentrations following intraperitoneal IL-12 injection. Using this dataset to estimate transport-related parameters allows us to have greater confidence in both our predicted serum and intraperitoneal IL-12 concentrations. Accordingly, we first estimated the parameters describing IL-12 transport from the intraperitoneal space to the blood by fitting our model to clinical trial data presented by Lenzi et al.[33] modified to represent intraperitoneal injection of IL-12. Our model was able to accurately fit both the intraperitoneal and serum IL-12 concentrations (**SI Text, Supplementary Figure S6**), giving us confidence in the estimated transport parameters.

Additionally, a standard PK model is unable to fit this data, further supporting the relevance of our model. Since this dataset only consisted of a single intraperitoneal infusion of IL-12, we used the

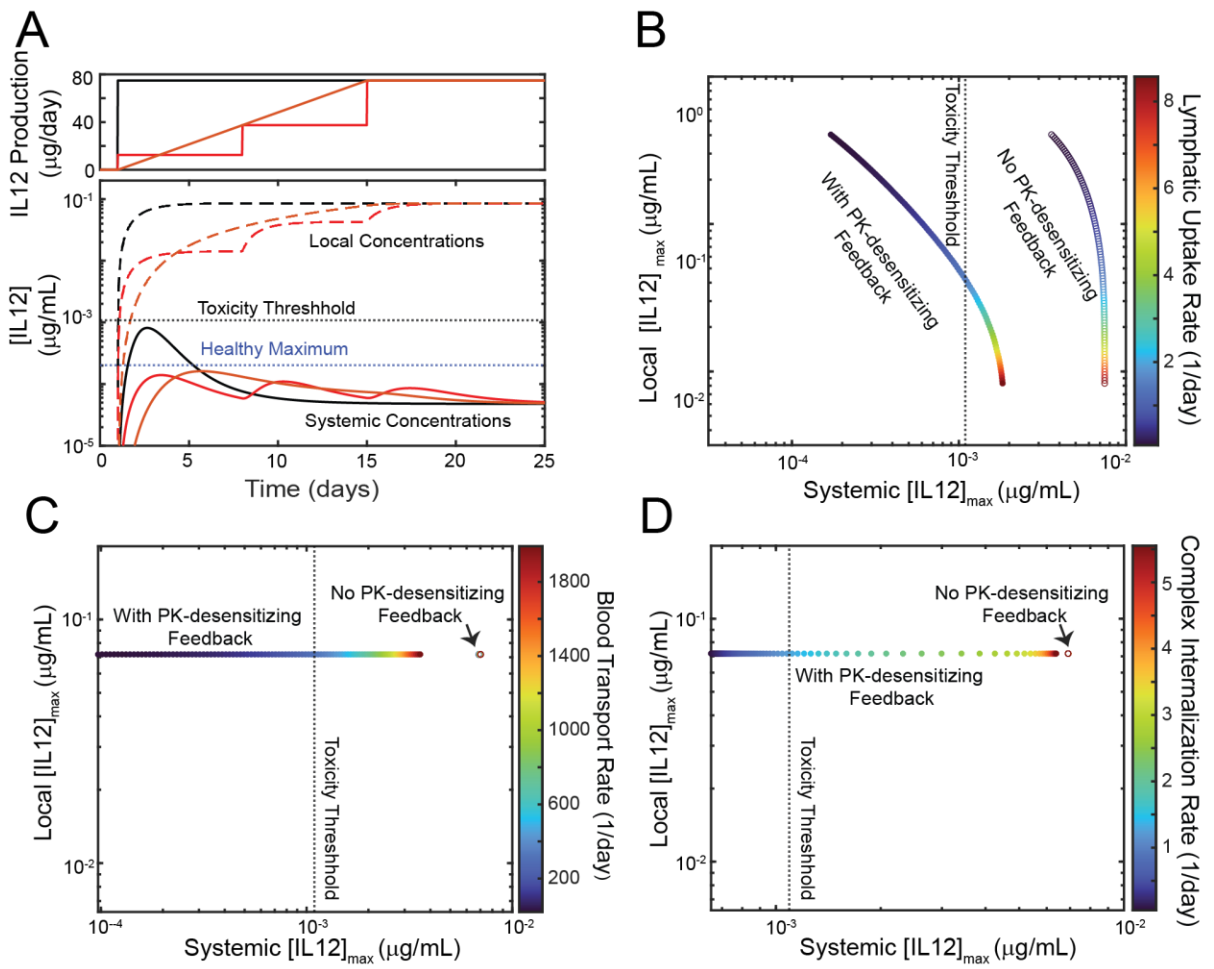

Figure 5: Model predictions of strategies for mitigating systemic IL-12 exposure following continuous local delivery. A) Prediction of continuous, intraperitoneal IL-12 delivery according to three different production rate profiles: constant production (black lines), step-wise production (red lines), and linearly increasing production (orange lines). Healthy IL-12 serum concentration taken from Derin et al.[34] B-D) Effects of various IL-12 related parameters on maximum concentrations in the local environment and in the blood. B) Effects of manipulating lymphatic uptake. C) Effects of limiting transport into the blood from the lymphatic system. C) Effects of limiting internalization of IL-12:IL-12 receptor complex.

transport parameters estimated from the Lenzi et al. data[33] and parameters to characterize receptor-upregulation feedback estimated from our fits in earlier sections.

299 We next used this model to simulate continuous IL-12 delivery to the peritoneal cavity and
300 predicted intraperitoneal and serum concentrations of IL-12 according to three different production
301 profiles: 1) constant production, 2) step-wise production, and 3) linearly-increasing production
302 (**Figure 5A**). All three production profiles were designed to reach an equivalent concentration of
303 IL-12 in the intraperitoneal space at steady state. Importantly, our model predicts serum IL-12
304 concentrations far above normal levels[34] following the constant production profile that does not
305 occur in either of the dynamic dosing strategies. Additionally, the concentration of IL-12 in the
306 intraperitoneal space at long times is indeed equivalent for all three strategies. These results
307 suggest that systemic exposure to IL-12 may be avoided following local delivery by utilizing
308 dosing strategies that slowly reach the desired production rate for local concentrations rather than
309 immediately starting at that level.

310 In addition to analyzing the predicted effects of dynamic dosing strategies, we used our model to
311 identify potential protein engineering approaches for limiting systemic exposure. Based on our
312 simulations, strategies modifying IL-12 to limit uptake into the lymphatic system from the local
313 environment (**Figure 5B**), limit uptake into the blood from the lymphatic system (**Figure 5C**), or
314 limit internalization of IL-12:receptor complex (**Figure 5D**) were predicted to have profound
315 effects due to our mechanism. We found that these aspects of IL-12 could be manipulated such
316 that the systemic exposure to IL-12 is reduced, and the concentrations in the local environment are
317 either increased or unchanged. These strategies are a direct result of IL-12 PK desensitization;
318 without our mechanism, they are not predicted to be effective. Ultimately, these results illustrate
319 how our proposed mechanism for IL-12 desensitization can be leveraged to identify strategies for
320 limiting systemic exposure to IL-12 treatment.

321 **Discussion**

322 Here, we employ a modeling approach to validate proposed mechanisms for IL-12 PK
323 desensitization. Two models of IL-12 PK containing feedback mechanisms causing increased
324 clearance or reduced bioavailability following repeated doses of IL-12 were developed. The
325 accelerated-clearance model failed to capture IL-12 PK accurately, whereas the reduced-
326 bioavailability model accurately fit IL-12 PK across three separate clinical trials. Ultimately, our
327 results allowed us to develop a model that can accurately predict IL-12 PK desensitization, which
328 is not currently available to the best of our knowledge.

329 The molecular mechanism we propose for IL-12 PK desensitization is that IL-12 stimulation of T-
330 cells in the lymphatic system leads to increased expression of the IL-12 receptor and IL-12
331 sequestration during transport into the blood. This mechanism is based on the observation in
332 literature that IL-12 activation of STAT4 in T-cells leads to increased IL-12 receptor expression in
333 both *in vitro* and *in vivo* experiments[19,21]. These studies illustrated the presence of this feedback
334 loop; however, its specific effects on IL-12 desensitization have yet to be fully elucidated. Our
335 results provide quantitative justification for how upregulation of IL-12 receptor affects IL-12 PK.
336 Given that our investigation is purely theoretical, these results remain a hypothesis; however, we
337 believe there is evidence that supports that this proposed mechanism for IL-12 PK is biologically
338 feasible. First, in clinical trials detailing repeated i.v. administration of IL-12, little to no IL-12
339 PK desensitization is observed[8,14], suggesting that the mechanism causing IL-12 PK
340 desensitization occurs to a more significant extent in peripheral tissues. Furthermore, because IL-
341 12's molecular weight is greater than 16 kDa, it cannot enter the blood through capillary diffusion
342 and must travel through the lymphatic system to enter the blood from peripheral tissue[23]. T-cells
343 are highly abundant in the lymphatic system[35]; therefore, during lymphatic transport, it is expected
344 that significant IL-12:IL-12 receptor interaction will occur. Together with the previously

mentioned upregulation of IL-12 receptor on T-cells following stimulation, these pieces of evidence support that our proposed mechanism is highly realistic.

We next sought to explore the implications of our proposed mechanism on the design of IL-12 therapies. The development of IL-12 therapies today focuses on local delivery of IL-12 through gene or cell-based therapies[9,10,13,18,36,37]. These technologies are designed to maintain high levels of IL-12 near the tumor while limiting systemic IL-12 exposure. Importantly, technologies where significant IL-12 exposure occurs cause severe toxicities, limiting the therapeutic window of treatment[37]. Based on these observations, we used our model to identify potential strategies leveraging IL-12 PK desensitization to maintain low levels of IL-12 exposure. We found that designing IL-12 therapies to begin with lower production rates and slowly increase until reaching the desired dose can prevent initial spikes in IL-12 exposure. Furthermore, we identified several protein engineering approaches that can be utilized to maximize concentrations in the local environment while limiting serum exposure to IL-12.

The molecular mechanism we suggest for IL-12 PK desensitization provides an example of how regulation of a biologic's target can influence the bioavailability of the therapeutic. Unlike small molecules, biologics are known to have complex PK due to their large molecular weights, strong binding to their targets, and connection between PK and PD[38]. The influence of target binding on biologic PK is known as target-mediated drug disposition (TMDD)[28]. More specifically, TMDD involves target-mediated clearance of the biologic, and since the abundance of targets is finite these effects become dose-dependent. Additionally, cases have been identified where a biologic upregulates the abundance of its target, leading to an increase in clearance[28]. For example, pegfilgrastim is a colony-stimulating factor targeting neutrophils, and activity leads to neutrophil proliferation. As a result, pegfilgrastim stimulation leads to increased target abundance and an

368 increase of drug clearance[39]. While these effects are typically related to increased clearance of a
369 biologic, our results provide a quantitative explanation for how target upregulation can also affect
370 bioavailability. Despite our focus on IL-12, our results provide insight into complex PK of other
371 biologics. In cases where a biologic's target is highly abundant in the lymphatic system and
372 upregulated by the biologic's action, we show that the bioavailability of the therapeutic can
373 decrease with repeated dosing.

374 **Study Highlights**

375 What is the current knowledge on this topic?

376 IL-12 desensitization was observed in the earliest clinical trials investigating IL-12
377 immunotherapy, and several studies have linked the phenomenon to treatment efficacy and
378 tolerability. Mechanisms have been hypothesized in literature, but none have been validated
379 quantitatively.

380 What question did this study address?

381 What is the desensitization mechanism capable of correctly predicting IL-12 pharmacokinetics
382 over repeated doses, and what are the therapeutic consequences of that mechanism?

383 What does this study add to our knowledge?

384 Here, we developed a mathematical model that attempts to validate the mechanisms causing IL-
385 12 PK desensitization in the absence of mechanistic data. Our results illustrate that IL-12 PK
386 desensitization is likely to be a result of decreased bioavailability after repeated exposure to IL-12
387 rather than increased systemic clearance. We propose a molecular mechanism for this model based
388 on the upregulation of IL-12 receptor on T-cells in the lymphatic system.

How might this change drug discovery, development, and/or therapeutics?

Pharmacokinetic modeling is essential in predicting the behavior of therapeutics in humans. We provide a tool for predicting IL-12 pharmacokinetics, which will undoubtedly aid in the development of IL-12 based therapies.

Author Contributions

J.D., O.A.I., and O.V. wrote the manuscript; J.D. and O.A.I. designed the research; J.D performed the research; J.D. and O.A.I. analyzed the data.

References

1. Cirella A, Luri-Rey C, Di Trani CA, et al. Novel strategies exploiting interleukin-12 in cancer immunotherapy. *Pharmacology & Therapeutics*. 2022;239:108189. doi:10.1016/j.pharmthera.2022.108189

2. Jalah R, Rosati M, Ganneru B, et al. The p40 Subunit of Interleukin (IL)-12 Promotes Stabilization and Export of the p35 Subunit. *J Biol Chem*. 2013;288(9):6763-6776. doi:10.1074/jbc.M112.436675

3. Hamza T, Barnett JB, Li B. Interleukin 12 a Key Immunoregulatory Cytokine in Infection Applications. *Int J Mol Sci*. 2010;11(3):789-806. doi:10.3390/ijms11030789

4. Berger A. Th1 and Th2 responses: what are they? *BMJ*. 2000;321(7258):424.

5. Gately MK, Renzetti LM, Magram J, et al. THE INTERLEUKIN-12/INTERLEUKIN-12-RECEPTOR SYSTEM: Role in Normal and Pathologic Immune Responses. *Annual Review of Immunology*. 1998;16(1):495-521. doi:10.1146/annurev.immunol.16.1.495

6. Athie-Morales V, Smits HH, Cantrell DA, Hilkens CMU. Sustained IL-12 Signaling Is Required for Th1 Development 1. *The Journal of Immunology*. 2004;172(1):61-69. doi:10.4049/jimmunol.172.1.61

7. Atkins MB, Robertson MJ, Gordon M, et al. Phase I evaluation of intravenous recombinant human interleukin 12 in patients with advanced malignancies. *Clin Cancer Res*. 1997;3(3):409-417.

8. Leonard JP, Sherman ML, Fisher GL, et al. Effects of Single-Dose Interleukin-12 Exposure on Interleukin-12–Associated Toxicity and Interferon-γ Production. *Blood*. 1997;90(7):2541-2548. doi:10.1182/blood.V90.7.2541

9. Algazi AP, Twitty CG, Tsai KK, et al. Phase II Trial of IL-12 Plasmid Transfection and PD-1 Blockade in Immunologically Quiescent Melanoma. *Clinical Cancer Research*. 2020;26(12):2827-2837. doi:10.1158/1078-0432.CCR-19-2217

10. Algazi A, Bhatia S, Agarwala S, et al. Intratumoral delivery of tavokinogene telseplasmid yields systemic immune responses in metastatic melanoma patients. *Ann Oncol*. 2020;31(4):532-540. doi:10.1016/j.annonc.2019.12.008

11. Bajetta E, Del Vecchio M, Mortarini R, et al. Pilot study of subcutaneous recombinant human interleukin 12 in metastatic melanoma. *Clinical Cancer Research*. 1998;4(1):75-85.

12. Bekaii-Saab TS, Roda JM, Guenterberg KD, et al. A phase I trial of paclitaxel and trastuzumab in combination with interleukin-12 in patients with HER2/neu-expressing malignancies. *Molecular Cancer Therapeutics*. 2009;8(11):2983-2991. doi:10.1158/1535-7163.MCT-09-0820

13. Bhatia S, Longino NV, Miller NJ, et al. Intratumoral Delivery of Plasmid IL12 Via Electroporation Leads to Regression of Injected and Noninjected Tumors in Merkel Cell Carcinoma. *Clinical Cancer Research*. 2020;26(3):598-607. doi:10.1158/1078-0432.CCR-19-0972

14. Gollob JA, Mier JW, Veenstra K, et al. Phase I Trial of Twice-Weekly Intravenous Interleukin 12 in Patients with Metastatic Renal Cell Cancer or Malignant Melanoma: Ability to Maintain IFN-γ Induction Is Associated with Clinical Response1. *Clinical Cancer Research*. 2000;6(5):1678-1692.

15. Motzer RJ, Rakhit A, Schwartz LH, et al. Phase I trial of subcutaneous recombinant human interleukin-12 in patients with advanced renal cell carcinoma. *Clinical Cancer Research*. 1998;4(5):1183-1191.

16. Portielje JEA, Kruit WHJ, Schuler M, et al. Phase I Study of Subcutaneously Administered Recombinant Human Interleukin 12 in Patients with Advanced Renal Cell Cancer. *Clinical Cancer Research*. 1999;5(12):3983-3989.

17. Portielje JEA, Lamers CHJ, Kruit WHJ, et al. Repeated Administrations of Interleukin (IL)-12 Are Associated with Persistently Elevated Plasma Levels of IL-10 and Declining IFN-γ, Tumor Necrosis Factor-α, IL-6, and IL-8 Responses. *Clinical Cancer Research*. 2003;9(1):76-83.

18. Barton KN, Siddiqui F, Pompa R, et al. Phase I trial of oncolytic adenovirus-mediated cytotoxic and interleukin-12 gene therapy for the treatment of metastatic pancreatic cancer. *Molecular Therapy - Oncolytics*. 2021;20:94-104. doi:10.1016/j.omto.2020.11.006

19. Rakhit A, Yeon MM, Ferrante J, et al. Down-regulation of the pharmacokinetic-pharmacodynamic response to interleukin-12 during long-term administration to patients with renal cell carcinoma and evaluation of the mechanism of this “adaptive response” in mice. *Clinical Pharmacology & Therapeutics*. 1999;65(6):615-629. doi:10.1016/S0009-9236(99)90083-8

20. Coughlin CM, Wysocka M, Trinchieri G, Lee WMF. The Effect of Interleukin 12 Desensitization on the Antitumor Efficacy of Recombinant Interleukin 121. *Cancer Research*. 1997;57(12):2460-2467.

21. Becskei A, Grusby MJ. Contribution of IL-12R mediated feedback loop to Th1 cell differentiation. *FEBS Letters*. 2007;581(27):5199-5206. doi:10.1016/j.febslet.2007.10.007

22. Wang KS, Zorn E, Ritz J. Specific down-regulation of interleukin-12 signaling through induction of phospho-STAT4 protein degradation. *Blood*. 2001;97(12):3860-3866. doi:10.1182/blood.V97.12.3860

23. Supersaxo A, Hein WR, Steffen H. Effect of Molecular Weight on the Lymphatic Absorption of Water-Soluble Compounds Following Subcutaneous Administration. *Pharm Res*. 1990;7(2):167-169. doi:10.1023/A:1015880819328

24. Datta-Mannan A. Mechanisms Influencing the Pharmacokinetics and Disposition of Monoclonal Antibodies and Peptides. *Drug Metab Dispos*. 2019;47(10):1100-1110. doi:10.1124/dmd.119.086488

25. Zhao L, Ren T hua, Wang DD. Clinical pharmacology considerations in biologics development. *Acta Pharmacol Sin*. 2012;33(11):1339-1347. doi:10.1038/aps.2012.51

26. Tibbitts J, Canter D, Graff R, Smith A, Khawli LA. Key factors influencing ADME properties of therapeutic proteins: A need for ADME characterization in drug discovery and development. *mAbs*. 2016;8(2):229-245. doi:10.1080/19420862.2015.1115937

27. Martin JP, Rasor BJ, DeBonis J, et al. A dynamic kinetic model captures cell-free metabolism for improved butanol production. *Metabolic Engineering*. 2023;76:133-145. doi:10.1016/j.ymben.2023.01.009

28. An G. Concept of Pharmacologic Target-Mediated Drug Disposition in Large-Molecule and Small-Molecule Compounds. *The Journal of Clinical Pharmacology*. 2020;60(2):149-163. doi:10.1002/jcph.1545

29. Bensalem A, Ternant D. Pharmacokinetic Variability of Therapeutic Antibodies in Humans: A Comprehensive Review of Population Pharmacokinetic Modeling Publications. *Clin Pharmacokinet*. 2020;59(7):857-874. doi:10.1007/s40262-020-00874-2

30. Thaker PH, Brady WE, Lankes HA, et al. A phase I trial of intraperitoneal GEN-1, an IL-12 plasmid formulated with PEG-PEI-cholesterol lipopolymer, administered with pegylated liposomal doxorubicin in patients with recurrent or persistent epithelial ovarian, fallopian tube or primary peritoneal cancers: An NRG Oncology/Gynecologic Oncology Group study. *Gynecologic Oncology*. 2017;147(2):283-290. doi:10.1016/j.ygyno.2017.08.001

31. Alvarez RD, Sill MW, Davidson SA, et al. A phase II trial of intraperitoneal EGEN-001, an IL-12 plasmid formulated with PEG–PEI–cholesterol lipopolymer in the treatment of persistent or recurrent epithelial ovarian, fallopian tube or primary peritoneal cancer: A

Gynecologic Oncology Group study. *Gynecologic Oncology*. 2014;133(3):433-438. doi:10.1016/j.ygyno.2014.03.571

32. Bella Á, Arrizabalaga L, Di Trani CA, et al. Intraperitoneal administration of a modified vaccinia virus Ankara confers single-chain interleukin-12 expression to the omentum and achieves immune-mediated efficacy against peritoneal carcinomatosis. *J Immunother Cancer*. 2023;11(11):e006702. doi:10.1136/jitc-2023-006702

33. Lenzi R, Rosenblum M, Verschraegen C, et al. Phase I Study of Intraperitoneal Recombinant Human Interleukin 12 in Patients with Müllerian Carcinoma, Gastrointestinal Primary Malignancies, and Mesothelioma1. *Clinical Cancer Research*. 2002;8(12):3686-3695.

34. Derin D, Soydinc HO, Guney N, et al. Serum IL-8 and IL-12 levels in breast cancer. *Medical Oncology*. 2007;24(2):163-168. doi:10.1007/BF02698035

35. Sender R, Weiss Y, Navon Y, et al. The total mass, number, and distribution of immune cells in the human body. *Proceedings of the National Academy of Sciences*. 2023;120(44):e2308511120. doi:10.1073/pnas.2308511120

36. Greaney SK, Algazi AP, Tsai KK, et al. Intratumoral Plasmid IL12 Electroporation Therapy in Patients with Advanced Melanoma Induces Systemic and Intratumoral T-cell Responses. *Cancer Immunology Research*. 2020;8(2):246-254. doi:10.1158/2326-6066.CIR-19-0359

37. Zhang L, Morgan RA, Beane JD, et al. Tumor-Infiltrating Lymphocytes Genetically Engineered with an Inducible Gene Encoding Interleukin-12 for the Immunotherapy of Metastatic Melanoma. *Clinical Cancer Research*. 2015;21(10):2278-2288. doi:10.1158/1078-0432.CCR-14-2085

38. Shi S. Biologics: An Update and Challenge of Their Pharmacokinetics. *Current Drug Metabolism*. 2014;15(3):271-290.

39. Roskos LK, Lum P, Lockbaum P, Schwab G, Yang BB. Pharmacokinetic/Pharmacodynamic Modeling of Pegfilgrastim in Healthy Subjects. *The Journal of Clinical Pharmacology*. 2006;46(7):747-757. doi:10.1177/0091270006288731

Figure Legends

Figure 1: Clinical trial dosing information and schematics of models used in this investigation. A) Timelines illustrating dose regimens and doses where blood measurements are taken in three clinical trials used in this investigation. B) Schematic of accelerated-clearance model. C) Schematic of reduced-bioavailability model.

Figure 2: Accelerated-clearance model fitness to clinical trial data with and without feedback. A) Accelerated-clearance model fit to clinical trial data presented by Motzer et al. B) Accelerated-clearance model fit to clinical trial data presented by Rakhit et al. Black arrows represent dose administration C) Accelerated-clearance model fit to IL-12 time course data following 1.0 μg/kg administration with no prior doses from Motzer et al. D) Accelerated-clearance model refit to IL-12 time course data 1.0 μg/kg administration with two prior doses from Motzer et al. All model parameters other than bioavailability and absorption (solid line) or systemic clearance rate (dashed line) fixed to values in C).

Figure 3: Reduced-bioavailability model fit to clinical trial data. A) Reduced-bioavailability model fit to clinical trial data presented by Motzer et al. after global optimization. B) Reduced-bioavailability model fit to clinical trial data presented by Rakhit et al. after global optimization. C) Distribution of generated ensemble fit to all three clinical trials following local optimization of randomly sampled parameter sets within boundaries (50 parameter sets per clinical trial).

Figure 4: Analysis of model and dosing parameters influence on predicted amounts of desensitization. A) Predicted amount of desensitization after two consecutive IL-12 doses seven days apart at varying dose levels. Inset: visual representation of AUC ratio. B) Predicted amount of desensitization after two consecutive 1.0 μg/kg doses with varying time between doses.

Figure 5: Model predictions of strategies for mitigating systemic IL-12 exposure following continuous local delivery. A) Prediction of continuous, intraperitoneal IL-12 delivery according to three different production rate profiles: constant production (black lines), step-wise production (red lines), and linearly increasing production (orange lines). Healthy IL-12 serum concentration taken from Derin et al.[34] B-D) Effects of various IL-12 related parameters on maximum concentrations in the local environment and in the blood. B) Effects of manipulating lymphatic

uptake. C) Effects of limiting transport into the blood from the lymphatic system. C) Effects of limiting internalization of IL-12:IL-12 receptor complex.

Supplementary Material

All supplementary tables, figures, and text are included in the attached file titled "Supplementary Information.pdf".

SUPPLEMENTARY INFORMATION FOR

Uncovering the Interleukin-12 Pharmacokinetic Desensitization and Its Consequences with Mathematical Modeling

Jonathon DeBonis, Omid Veiseh, and Oleg Igoshin

Oleg Igoshin

Email: igoshin@rice.edu

All MATLAB code used in this investigation can be found at the following GitHub repository: https://github.com/jcd111/IL-12-PK-Desensitization-Model

This PDF file includes:

Supplementary Tables S1 to S7	S2
Supplementary Figures S1 to S8	S8
List of Mathematical Models and Equations	S14
Supplementary Text	S18
Supplementary References	S31

Supplemental Table S1: Reported IL-12 C_{max}, AUC, and t_{max} by Portielje et al. following repeated s.c. injections compared to accelerated-clearance model predictions after global optimization. Predicted values are reported to two significant digits.

Dose Information	Predicted C_{max}	Reported C_{max}	Predicted AUC	Reported AUC	Predicted t_{max}	Reported t_{max}
0.5 $\mu g/kg$, dose 1	430 pg/mL	362 (214) pg/mL	8,200 pg*h/mL	7,400 (5,400) pg*h/mL	5.1 h	9.7 (5) h
0.5 $\mu g/kg$, dose 7	250 pg/mL	255 (200) pg/mL	4,000 pg*h/mL	3,300 (1,600) pg*h/mL	2.8 h	9.5 (2.2) h
1.0 $\mu g/kg$, dose 1	1000 pg/mL	1131 (1051) pg/mL	22,000 pg*h/mL	31,800 (22,300) pg*h/mL	8.4 h	17 (7) h
1.0 $\mu g/kg$, dose 7	360 pg/mL	376 (49) pg/mL	5,600 pg*h/mL	6,000 (2,400) pg*h/mL	2.3 h	4 (0) h

*Values in () are reported standard deviation.

Supplemental Table S2: Accelerated-clearance model parameter values following global optimization to three clinical trials individually. Values are reported to two significant digits.

Parameter	Value fit to Motzer data	Value fit to Rakhit data	Value fit to Portielje data
k_{CB} (days^{-1})	0.80	0.80	0.80
k_{CR} (days^{-1})	0.75	0.46	0.46
k_{on}(mL pmol^{-1}days^{-1})	200	200	210
k_{int}(days^{-1})	0.49	0.49	0.46
α (days^{-1})	3.5e-6	3.9e-6	2.8e-6
F (unitless)	0.83	0.41	0.60
J_{BS} (days^{-1})	0.25	0.27	1.2
R_0 (pmol/cell)	1.8e-9	1.7e-9	6.7e-9
N_B(cells)	4.2e10	4.2e10	5.2e10
IC_{pSTAT} (#/cell)	6.6e5	8.2e5	1.8e6

Supplemental Table S3: Reported IL-12 C_{max}, AUC, and t_{max} by Portielje et al. following repeated s.c. injections compared to reduced-bioavailability model predictions after global optimization. Predicted values are reported to two significant digits.

Dose Information	Predicted C_{max}	Reported C_{max}	Predicted AUC	Reported AUC	Predicted t_{max}	Reported t_{max}
0.5 μg/kg, dose 1	330 pg/mL	362 (214) pg/mL	7,400 pg*h/mL	7,400 (5,400) pg*h/mL	10 h	9.7 (5) h
0.5 μg/kg, dose 7	170 pg/mL	255 (200) pg/mL	4,100 pg*h/mL	3,300 (1,600) pg*h/mL	10 h	9.5 (2.2) h
1.0 μg/kg, dose 1	1,300 pg/mL	1131 (1051) pg/mL	26,000 pg*h/mL	31,800 (22,300) pg*h/mL	9.8 h	17 (7) h
1.0 μg/kg, dose 7	290 pg/mL	376 (49) pg/mL	6,800 pg*h/mL	6,000 (2.4) pg*h/mL	10 h	4 (0) h

*Values in () are reported standard deviation.

Supplemental Table S4: Reduced-bioavailability model parameter values following global optimization to three clinical trials individually. Values are reported to two significant digits.

Parameter	Value fit to Motzer data	Value fit to Rakhit data	Value fit to Portielje data
$k_{CB}(\text{days}^{-1})$	1.6	2.4	2.4
$k_{CR}(\text{days}^{-1})$	0.46	0.50	1.7
$k_{on}(\text{mL pmol}^{-1}\text{days}^{-1})$	200	200	200
$k_{int}(\text{days}^{-1})$	0.56	0.59	0.66
$N_L(\text{cells})$	3.8e10	3.3e10	1.7e11
$\alpha(\text{pmol cells}^{-1}\text{days}^{-1})$	5.0e-6	3.1e-6	4.4e-6
R_0 (pmol cells^{-1})	5.6e-9	5.5e-9	1.8e-9
J_{LS} (days^{-1})	1.6	1.2	2.9
J_{BL} (days^{-1})	70	130	150
IC_{pstat} (# cells^{-1})	1.4e6	9.8e5	1.8e6

Supplemental Table S5: Reported IL-12 C_{max}, AUC, and t_{max} by Portielje et al. following repeated s.c. injections compared to reduced-bioavailability model predictions after ensemble local optimization. Predicted values are reported to two significant digits.

Dose Information	Predicted C_{max}	Reported C_{max}	Predicted AUC	Reported AUC	Predicted t_{max}	Reported t_{max}
0.5 μg/kg, dose 1	350 (30) pg/mL	362 (214) pg/mL	8,700 (570) pg*h/mL	7,400 (5,400) pg*h/mL	9.6 (1.1) h	9.7 (5) h
0.5 μg/kg, dose 7	170 (15) pg/mL	255 (200) pg/mL	4,500 (180) pg*h/mL	3,300 (1,600) pg*h/mL	9.7 (0.86) h	9.5 (2.2) h
1.0 μg/kg, dose 1	940 (190) pg/mL	1131 (1051) pg/mL	21,000 (4,200) pg*h/mL	31,800 (22,300) pg*h/mL	9.3 (1.1) h	17 (7) h
1.0 μg/kg, dose 7	240 (20) pg/mL	376 (49) pg/mL	6,300 (290) pg*h/mL	6,000 (2,400) pg*h/mL	9.8 (0.94) h	4 (0) h

*Values in () are reported/estimated standard deviation.

Supplemental Table S6: Accelerated-clearance model parameter information.

Parameter	Meaning	Optimization Range/Default Value	Source
J_{BS} (days^{-1})	First order transport rate for IL-12 to the blood.	1.0e-4 – 5.0	Estimated, given large range.
k_{CB} (days^{-1})	IL-12 first order clearance rate from blood.	0.79 – 2.4	Reported half-life values in clinical trials (Motzer et al.[1], Rakhit et al.[2], Portielje et al.[3])
k_{DG} (days^{-1})	First order degradation rate of IL-12 in the blood.	n/a	Determined by equation S8
F (unitless)	Absolute bioavailability, fraction of	0.010 – 1.0	Estimated, given range of reasonable values.

	administered IL-12 reaching blood.		
k_{on}(mL pmol^{-1}days^{-1})	IL-12 IL-12 receptor association rate.	1.5 – 210	Chizzonite et al.[4], adjusted to have high binding rate for improved fit to data.
k_R(pmol cells^{-1}days^{-1})	Basal receptor production rate.	n/a	Determined by equation S7
k_{CR} (days^{-1})	IL-12 receptor unbound internalization rate	0.46 – 1.1	Literature estimate unavailable, estimated based on half life between 10 and 36 hours.
k_{int}(days^{-1})	IL-12 receptor bound internalization rate.	0.46 – 1.1	Literature estimate unavailable, estimated based on half life between 10 and 36 hours.
α(pmol cells^{-1}days^{-1})	Linear feedback coefficient.	1.0e-8 – 1.0e-5	Estimated, given large range.
IC_{pSTAT}(# cells^{-1})	Complex formation required for 50% maximum STAT4 activation.	9.1e2 – 1.8e6	Estimated, given large range.
N_B(cells)	Number of IL-12R+ T-cells in the blood	8e8 – 8e10	Sender et al.[5]
R_0(pmol cells^{-1})	Initial amount of receptor per T-cell in lymphatic system.	1.7e-9 – 1.5e-8	Chizzonite et al[4].
$IL12_{S,0}$ (pmol mL^{-1})	Initial concentration of IL-12 in the subcutaneous space.	n/a	Determined by equation S9
D(pmol)	Dose amount.	n/a	Given based on dose information.
V_S (mL)	Volume of injection in subcutaneous space.	n/a	Based on volume of injection for clinical trials. Assumed to be 1 mL if not specified
V_B (mL)	Volume of the blood.	5100	Assumed as average human blood volume.

Supplemental Table S7: Reduced-bioavailability model parameter information.

Parameter	Meaning	Optimization Range/Default Value	Sources
$J_{LS}(\text{days}^{-1})$	First order IL-12 transport rate from subcutaneous space to lymphatic system.	0.79 – 2.4	Milewski et al.[6]
J_{BL} (days^{-1})	First order IL-12 transport rate from lymphatic system to blood.	4.3 – 430	Bounds centered around value reported by Varkhede et al.[7]
k_{CB} (days^{-1})	First order IL-12 clearance rate from blood.	0.79 – 2.4	Reported half-life values in clinical trials (Motzer et al.[1], Rakhit et al.[2], Portielje et al.[3])
$k_{DG}(\text{days}^{-1})$	First order degradation rate of IL-12 in the subcutaneous space.	n/a	Determined by equation S18.
$F(\text{unitless})$	Absolute bioavailability, fraction of IL-12 reaching lymphatic system.	1	Assumed to be one to isolate bioavailability mechanism.
k_{on} $(\text{mL pmol}^{-1}\text{days}^{-1})$	IL-12:IL-12 receptor association rate.	1.5 – 210	Chizzonite et al.[4], adjusted to have high binding rate for improved fit to data.
$k_R(\text{pmol cells}^{-1}\text{days}^{-1})$	Basal receptor production rate.	n/a	Determined by equation S17.
k_{CR} (days^{-1})	IL-12 receptor unbound internalization rate.	0.46– 1.7	Literature estimate unavailable, estimated based on half life between 10 and 36 hours.
k_{int} (days^{-1})	IL-12 receptor bound internalization rate.	0.46 – 1.7	Literature estimate unavailable, estimated based on half life between 10 and 36 hours.
$\alpha(\text{pmol cells}^{-1}\text{days}^{-1})$	Linear feedback coefficient.	1.0e-8 – 1.0e-5	Estimated, given large range.

$IC_{pSTAT}(\#\ \text{cells}^{-1})$	Complex formation required for 50% maximum STAT4 activation.	9.1e2 – 1.8e6	Estimated, given large range.
$N_L(\text{cells})$	Number of IL-12R+ T-cells in the lymphatic system	1.0e9 – 5.0e11	Sender et al.[5]
$R_0(\text{pmol cells}^{-1})$	Initial amount of receptor per T-cell in lymphatic system.	1.7e-9 – 1.5e-8	Chizzonite et al[4].
$IL12_{S,0}$ (pmol mL^{-1})	Initial concentration of IL-12 in the subcutaneous space.	n/a	Determined by equation S19.
$D(\text{pmol})$	Dose of IL-12 administered	Variable based on clinical trial.	Based on clinical trial information.
V_S (mL)	Volume of injection in subcutaneous space.	Variable based on clinical trial.	Based on volume of injection for clinical trials. Assumed to be 1 mL if not specified
V_L (mL)	Volume of lymphatic system IL-12 enters in transport to blood.	33	Varkhede et al.[7]
V_B (mL)	Volume of blood.	5100	Average human blood volume.

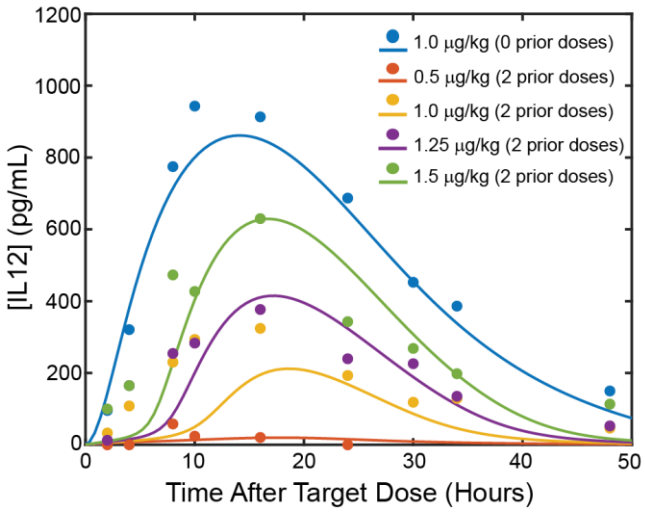

Supplemental Figure S1: Addition of IL-12 receptor binding and upregulation in the blood compartment to the reduced-bioavailability model allows for capturing non-linearity in dose escalation.

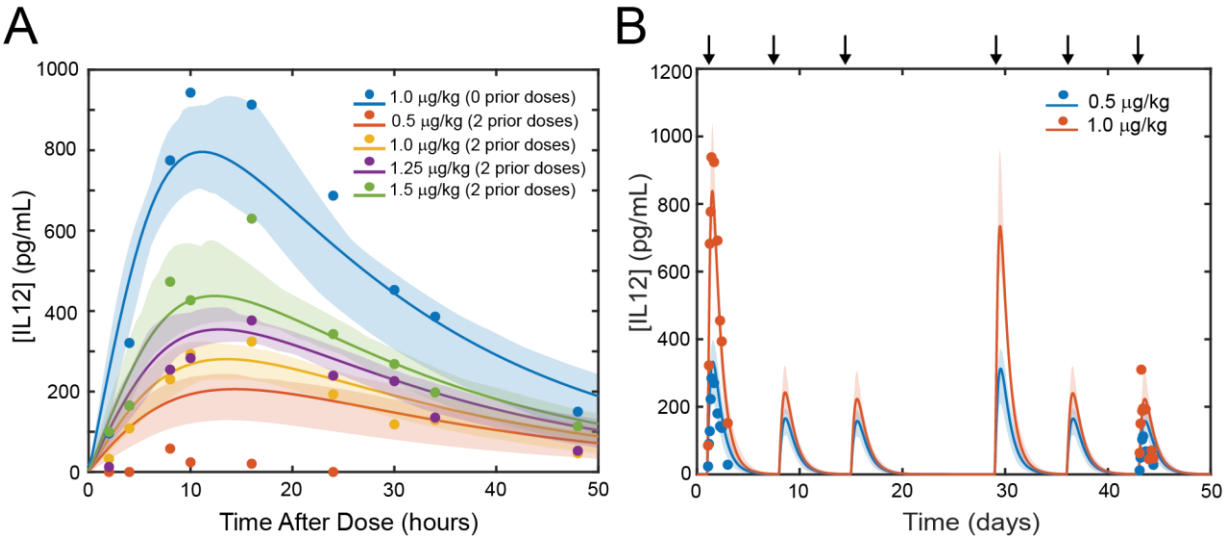

Supplemental Figure S2: Reduced-bioavailability model fitness to clinical trial data following ensemble-based optimization. A) Model predictions fit to clinical trial data presented by Motzer et al.[1]. B) Model predictions fit to clinical trial data presented by Rakhit et al.[2]. Solid lines: mean predicted concentrations. Shaded area: raw 95% confidence interval.

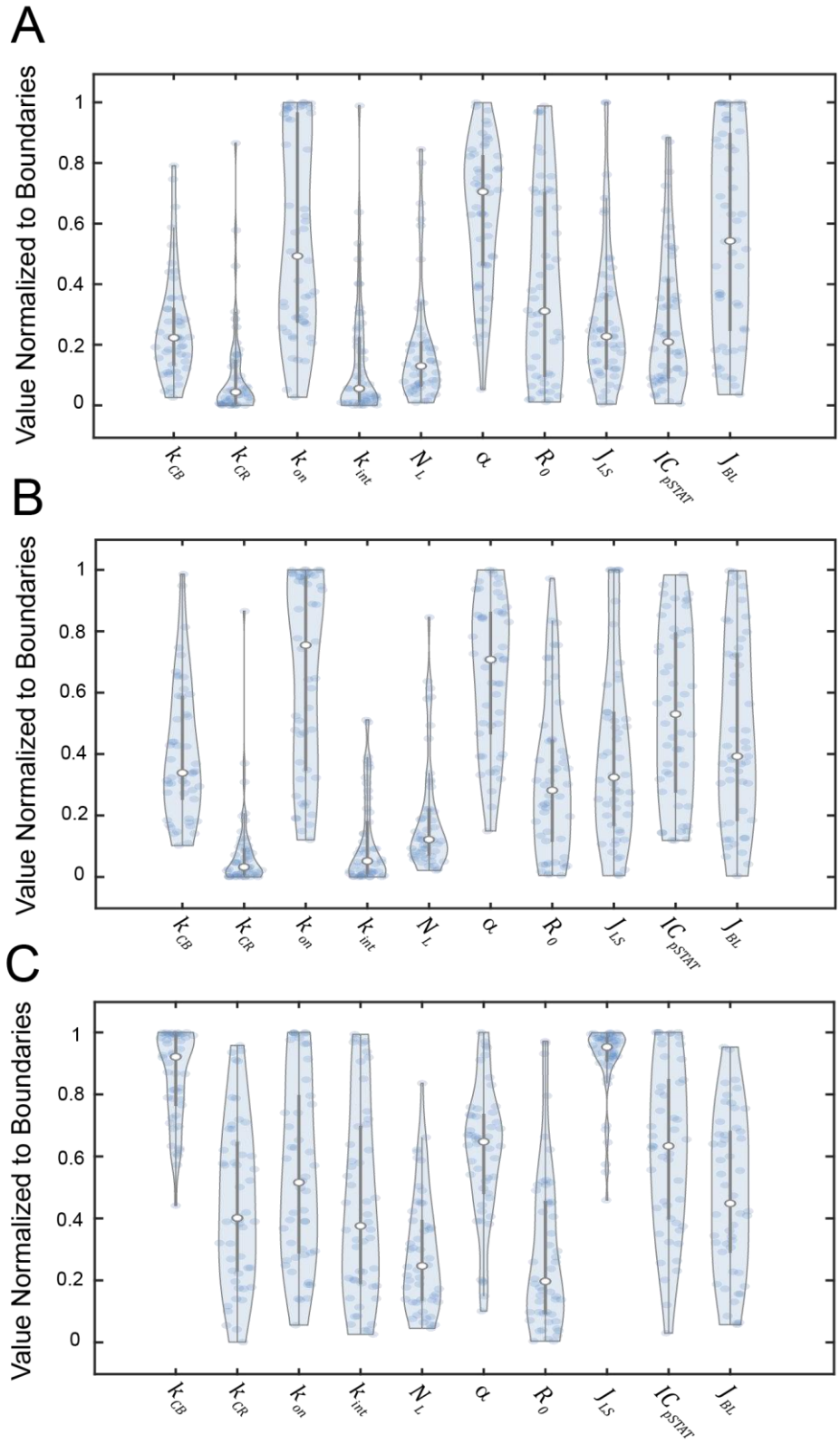

Supplemental Figure S3: Distribution of locally optimized parameters fit to individual clinical trials. A) Distribution of 50 parameter sets locally optimized to Motzer et al.[1] data. B)

Distribution of 50 parameter sets locally optimized to Rakhit et al.[2] data. C) Distribution of 50 parameter sets locally optimized to Portielje et al.[3] data.

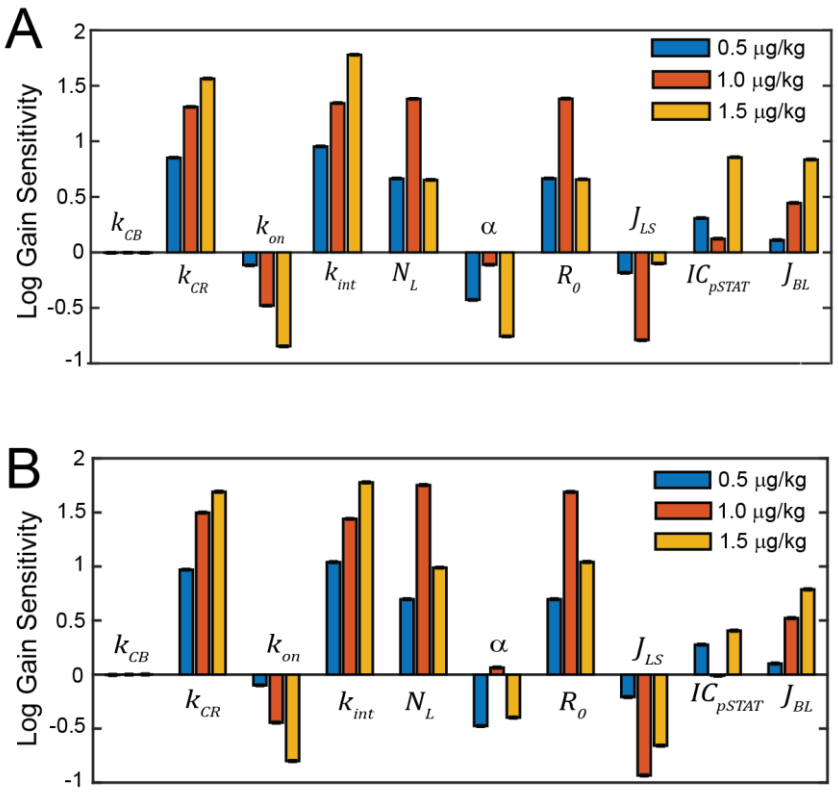

Supplemental Figure S4: Amount of desensitization predicted by reduced-bioavailability model sensitivities to relevant model parameters. A) Desensitization log gain sensitivities after two consecutive 1.0 μg/kg doses. B) Desensitization log gain sensitivities comparing desensitization after three consecutive 1.0 μg/kg doses. Sensitivities are calculated according to equation S64.

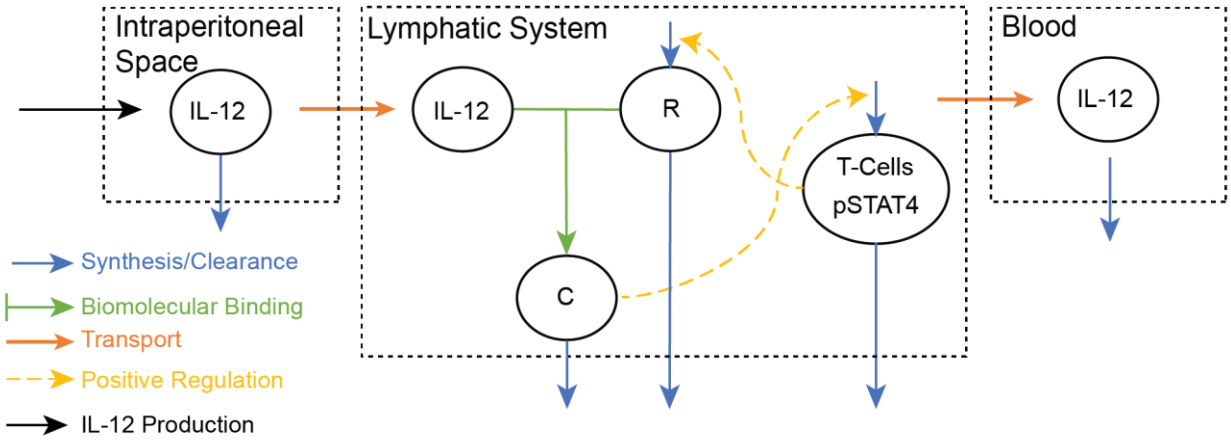

Supplemental Figure S5: Schematic of local IL-12 production model. This model is identical to the reduced-bioavailability model with the dosing compartment volume, method of dosing, and transport parameters modified to represent continuous IL-12 production in the i.p. space.

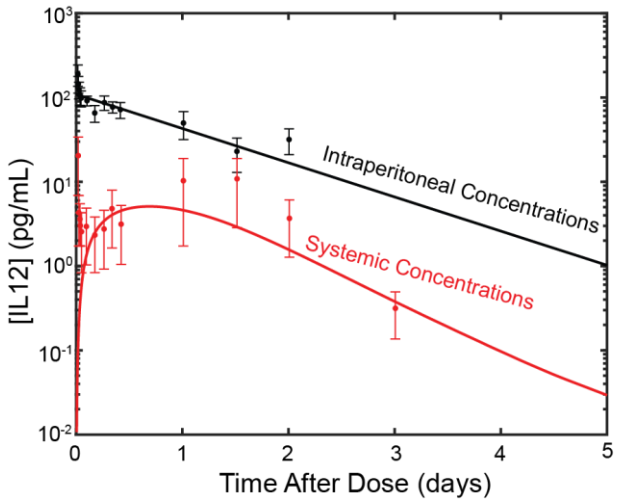

Supplemental Figure S6: Reduced-bioavailability model modified to represent IP injection of IL-12 fit to clinical trial data.

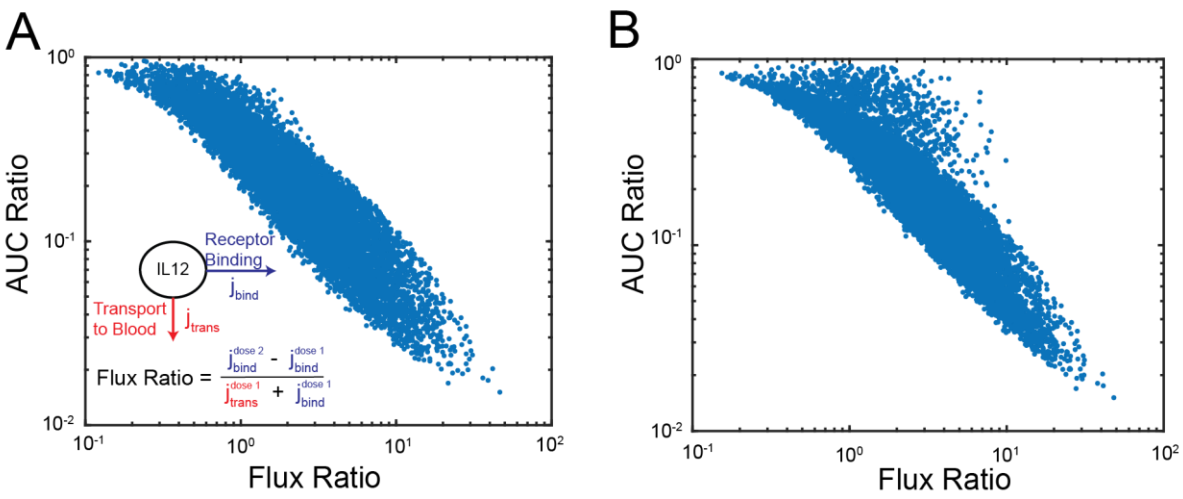

Supplemental Figure S7: Relationship between binding flux ratio and amount of desensitization predicted by AUC ratio. A) Predicted amount of desensitization as quantified by AUC ratio v. flux ratio determined from numerical simulations. Inset: visual representation of flux ratio. B) Predicted amount of desensitization as quantified by AUC ratio v. flux ratio determined by analytical approximation of receptor dynamics.

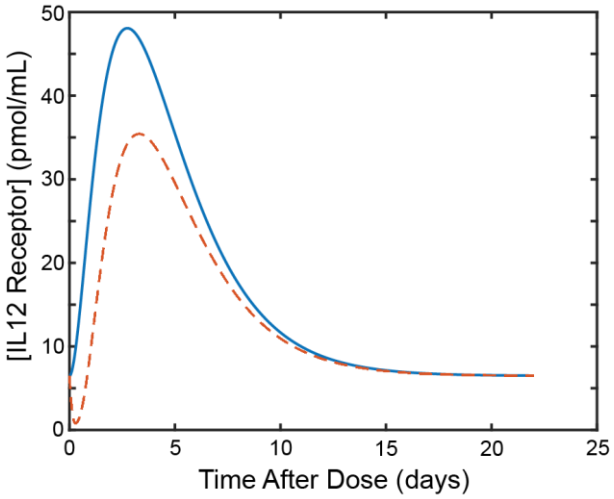

Supplemental Figure S8: Analytical approximation for receptor concentrations compared to numerical simulations for reduced-bioavailability model. Solid blue curve: analytical approximation. Dashed orange curve: numerical simulations.

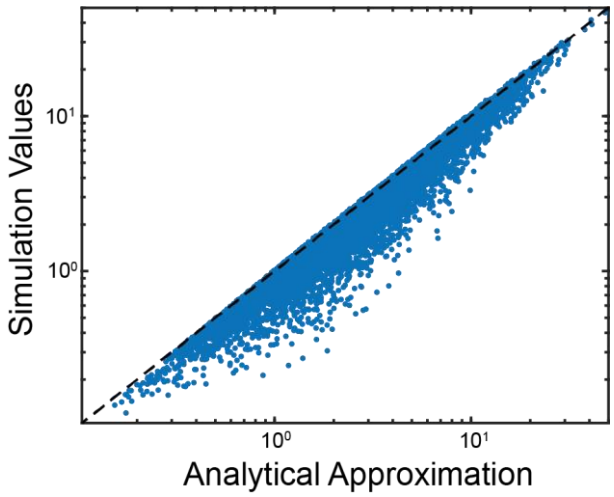

Supplemental Figure S9: Comparison of determined IL-12 binding flux ratio (equations S65 and S66) as calculated by numerical simulation and our analytical approximation for receptor dynamics.

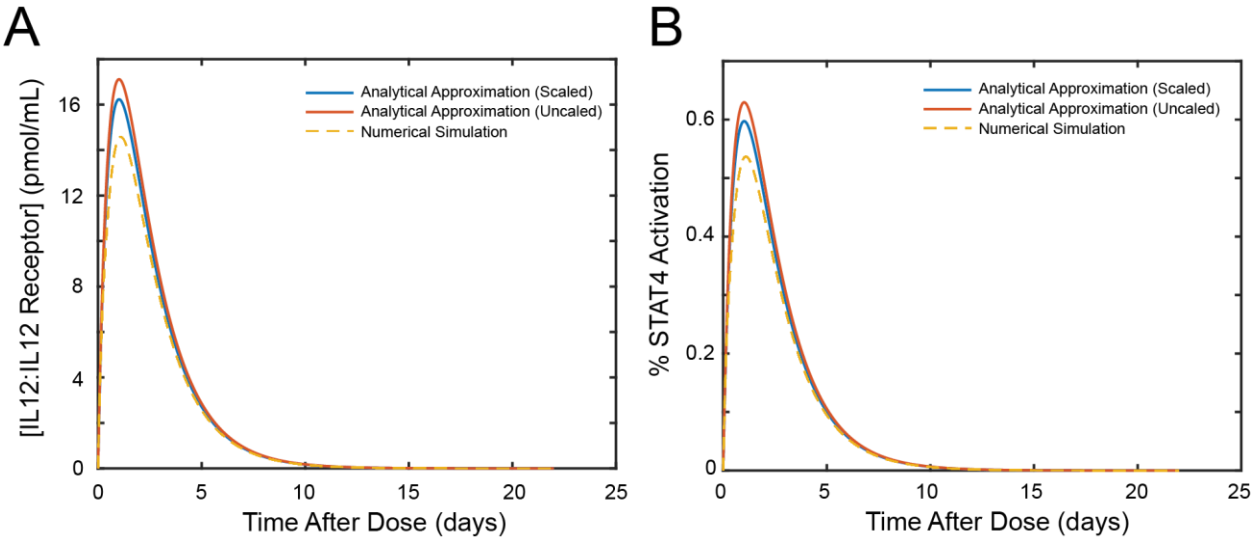

Supplemental Figure S10: Comparison of analytical approximation for the concentration of IL-12:IL-12 receptor and STAT4 activation in the reduced-bioavailability model. A) Predictions of complex concentrations. B) Predictions of STAT4 Activation. Blue curves: Scaled analytical approximations. Orange Curves: Unscaled analytical approximations. Dashed yellow curves: Numerically simulated values. See supplemental text for more information.

List of Mathematical Models and Equations

Accelerated-Clearance Model Equations

$$\frac{dIL12_S}{dt} = -J_{BS}\, IL12_S - k_{DG}\, IL12_S \tag{S1}$$

$$\frac{dIL12_B}{dt} = \frac{J_{BS}\, V_S}{V_B}\, IL12_S - k_{on}\, IL12_B\, R_B - k_{CB}\, IL12_B \tag{S2}$$

$$\frac{dR_B}{dt} = \frac{N_B}{V_B}\, k_R + \frac{N_B}{V_B}\, \alpha\, pSTAT_B - k_{on}\, IL12_B\, R_B - k_{CR}\, R_B \tag{S3}$$

$$\frac{dC_B}{dt} = k_{on}\, IL12_B\, R_B - k_{int}\, C_B \tag{S4}$$

$$\widetilde{C_B} = \frac{6.023e11\, V_B}{N_B}\, C_B \tag{S5}$$

$$pSTAT_B = \frac{\widetilde{C_B}}{\widetilde{C_B} + IC_{pSTAT}} \tag{S6}$$

$$k_R = k_{CR}\, R_0 \tag{S7}$$

$$k_{DG} = \frac{(1-F)}{F}\, J_{BS} \tag{S8}$$

$$IL12_{S,0} = \frac{D}{V_S} \tag{S9}$$

Reduced-Bioavailability Model Equations

$$\frac{dIL12_S}{dt} = -J_{LS} IL12_S - k_{DG} IL12_S \tag{S10}$$

$$\frac{dIL12_L}{dt} = \frac{J_{LS}\, V_S}{V_L}\, IL12_S - k_{on}\, IL12_L\, R_L - J_{BL}\, IL12_L \tag{S11}$$

$$\frac{dR_L}{dt} = \frac{N_L}{V_L}\, k_R + \frac{N_L}{V_L}\, \alpha\, pSTAT_L - k_{on}\, IL12_L\, R_L - k_{CR}\, R_L \tag{S12}$$

$$\frac{dC_L}{dt} = k_{on}\, IL12_L\, R_L - k_{int}\, C_L \tag{S13}$$

$$\frac{dIL12_B}{dt} = \frac{J_{BL}\, V_L}{V_B}\, IL12_L - k_{CB}\, IL12_B \tag{S14}$$

$$\widetilde{C_L} = \frac{6.023e11\, V_L}{N_L}\, C_L \tag{S15}$$

$$pSTAT_L = \frac{\tilde{C}_L}{\tilde{C}_L + IC_{pSTAT}} \tag{S16}$$

$$k_R = k_{CR}\, R_0 \tag{S17}$$

$$k_{DG} = \frac{(1-F)}{F}\, J_{LS} \tag{S18}$$

$$IL12_{S,0} = \frac{D}{V_S} \tag{S19}$$

Intraperitoneal Injection Model Equations

$$\frac{dIL12_P}{dt} = -J_{LP}\, IL12_P - k_{DG}\, IL12_P \tag{S20}$$

$$\frac{dIL12_L}{dt} = \frac{J_{LP} V_P}{V_L}\, IL12_P - k_{on}\, IL12_L\, R_L - J_{BL}\, IL12_L \tag{S21}$$

$$\frac{dR_L}{dt} = \frac{N_L}{V_L} k_R + \frac{N_L}{V_L}\, \alpha\, pSTAT_L - k_{on} IL12_L R_L - k_{CR} R_L \tag{S22}$$

$$\frac{dC_L}{dt} = k_{on}\, IL12_L\, R_L - k_{int} C_L \tag{S23}$$

$$\frac{dIL12_B}{dt} = \frac{J_{BL}V_L}{V_B}\, IL12_L - k_{CB}\, IL12_B \tag{S24}$$

$$\widetilde{C_L} = \frac{6.023e11V_L}{N_L} C_L \tag{S25}$$

$$pSTAT_L = \frac{\tilde{C}_L}{\widetilde{C_L} + IC_{pSTAT}} \tag{S26}$$

$$k_R = k_{CR}R_0 \tag{S27}$$

$$k_{DG} = \frac{(1-F)}{F} J_{LS} \tag{S28}$$

$$IL12_{P,0} = \beta \frac{D}{V_P} \tag{S29}$$

Local Production Model Equations

$$\frac{dIL12_P}{dt}\, k_{pr}(t) - J_{LP}\, IL12_P - \, k_{DG}\, IL12_P \tag{S30}$$

$$\frac{dIL12_L}{dt} = \frac{J_{LP}V_P}{V_L}\, IL12_P - k_{on}\, IL12_L\, R_L - J_{BL}\, IL12_L \tag{S31}$$

$$\frac{dR_L}{dt} = \frac{N_L}{V_L} k_R + \frac{N_L}{V_L}\, \alpha\, pSTAT_L - k_{on} IL12_L R_L - k_{CR} R_L \tag{S32}$$

$$\frac{dC_L}{dt} = k_{on}\, IL12_L\, R_L - k_{int} C_L \tag{S33}$$

$$\frac{dIL12_B}{dt} = \frac{J_{BL}V_L}{V_B}\, IL12_L - k_{CB}\, IL12_B \tag{S34}$$

$$\widetilde{C_L} = \frac{6.023e11V_L}{N_L} C_L \tag{S35}$$

$$pSTAT_L = \frac{\widetilde{C_L}}{\widetilde{C_L} + IC_{pSTAT}} \tag{S36}$$

$$k_R = k_{CR} R_0 \tag{S37}$$

$$k_{DG} = \frac{(1 - F)}{F} J_{LS} \tag{S38}$$

Supplementary Text

Contents

1. Derivation of Mathematical Models S19
   - 1.1 IL-12 Dosing S19
   - 1.2 IL-12 Transport Between Compartments S19
   - 1.3 IL-12 Receptor Binding and Complex Formation S21
   - 1.4 STAT4 Activation S21
   - 1.5 IL-12 Receptor Dynamics S22
   - 1.6 IL-12 Clearance S23
2. Model of Intraperitoneal IL-12 Injection S24
3. Model of Continuous, Local IL-12 Delivery S24
4. Parameter Optimization Error Functions S26
5. Local Model Sensitivity Analyses S27
6. Ensemble Analysis of Desensitization Requirements S27
7. Derivation of Analytical Approximation for Receptor Dynamics S29

Derivation of Mathematical Models

The models used in this investigation are based on the same principles. The accelerated-clearance model consists of subcutaneous and serum compartments with receptor dynamics in the serum compartment. Similarly, the reduced-bioavailability model consists of the same two compartments with the addition of a lymphatic system compartment where IL-12 must travel before reaching the blood and receptor binding occurs. The models used for the simulation of intraperitoneal IL-12 delivery are extensions of the reduced-bioavailability model. The equations governing IL-12 dosing, transport, clearance, binding, and signaling are equivalent for both models. In the following sections, we derive these terms. The descriptions and values for the parameters used in each model are located in **Supplemental Tables S6 and S7**.

IL-12 Dosing

In both models, IL-12 dosing occurs in the subcutaneous compartment. As the duration of injections is negligible compared to the simulation period, we model IL-12 dosing by setting the initial concentration of IL-12 in the subcutaneous space according to the following:

$$IL12_{S,0} = \frac{D}{V_S} \tag{S39}$$

Here, D is the dose amount administered in pmol and V_S is the volume of the subcutaneous space in mL.

IL-12 Transport Between Compartments

IL-12 transport between compartments is modeled based on a mass balance around each compartment and convective transport via lymph fluid flow. As the molecular weight of IL-12 is greater than 16 kDa, transport to the blood from the subcutaneous space primarily occurs through

lymph flow[8] and, therefore, is unidirectional. Consider a simple two-compartment system where lymph flow moves from compartment 1 to compartment 2 with a volumetric flow rate j_{21} in mL days^{-1}. The mass balance around these two compartments is given by:

$$\frac{dV_1C_1}{dt} = -j_{21}C_1 \tag{S40}$$

$$\frac{dV_2C_2}{dt} = j_{21}C_1 \tag{S41}$$

where V_i is the volume of compartment *i* in mL and C_i is the concentration of IL-12 in compartment *i* in pmol mL^{-1}. We assume that the volume of each compartment remains constant, i.e., fluid moving from each compartment is instantly replaced or removed. Accordingly, we can rearrange the two differential equations to become:

$$\frac{dC_1}{dt} = -\frac{j_{21}}{V_1}C_1 \tag{S42}$$

$$\frac{dC_2}{dt} = \frac{j_{21}}{V_2}C_2 \tag{S43}$$

Making the substitution $j_{21} = J_{21}V_1$, we further simplify to:

$$\frac{dC_1}{dt} = -J_{21}C_1 \tag{S44}$$

$$\frac{dC_2}{dt} = \frac{V_1}{V_2}J_{21}C_2 \tag{S45}$$

In these equations, J_{21} is the effective first order transport rate constant in days^{-1}. Conceptually, this parameter refers to the fluid flow leaving compartment 1 normalized by the volume of compartment 1. This framework is generalized to represent transport between all compartments in our model.

IL-12 Receptor Binding and Complex Formation

IL-12 binds its receptor either in the serum (accelerated-clearance model) or the lymphatic system (reduced-bioavailability model). For simplicity, we assume that binding is irreversible and occurs according to the rate law:

$$r_{binding} = k_{on}\ IL12_i\ R_i \tag{S46}$$

Here, k_{on} is the IL-12:IL-12 receptor association rate in mL pmol^{-1} days^{-1}, $IL12_i$ is the concentration of IL-12 in compartment *i* where receptor binding occurs, and R_i is the concentration of receptor in compartment *i* both in pmol mL $^{-1}$. In our model both IL-12 and IL-12 receptor are consumed according to $r_{binding}$, and IL-12:IL-12 complex is generated at the same rate. Accordingly, the differential equation describing the concentration of IL-12:IL-12 receptor complex is given by:

$$\frac{dC_i}{dt} = k_{on}\, IL12_i\, R_i - k_{int} C_i \tag{S47}$$

Here, C_i is the concentration of IL-12:IL-12 receptor complex in compartment *i* and k_{int} is the first order complex internalization rate constant in days^{-1}.

STAT4 Activation

In both models, the formation of IL-12:IL-12 receptor complex leads to the activation of STAT4 based on the number of complexes per T-cell. Accordingly, we first calculate this quantity according to:

$$\widetilde{C_i} = 6.023e11 \frac{V_i C_i}{N_i} \tag{S48}$$

where $\tilde{C}_i$ is the number of complexes per T-cell in # cells^{-1} in compartment i, V_i is the volume of compartment i in mL, and N_i is the number of T-cells in compartment i. The differential equation describing STAT4 activation is given by the following:

$$\frac{dpSTAT_i}{dt} = k_P \tilde{C}_i (1 - pSTAT_i) - k_{DP}\, pSTAT_i \tag{S49}$$

Here, $pSTAT_i$ is the fraction of phosphorylated (activated) STAT4, k_p is the first order phosphorylation rate in cell #$^{-1}$ days^{-1}, and k_{DP} is the first order dephosphorylation rate constant in days^{-1}. Furthermore, as intracellular processes are much faster than physiological processes such as transport and clearance, we assume that STAT4 activation is in quasi-steady state in our models. Thus, we can solve for $pSTAT_i$ activation as the following:

$$pSTAT_i = \frac{k_P \widetilde{C_\iota}}{k_P \widetilde{C_\iota} + k_{DP}} = \frac{\widetilde{C_\iota}}{\tilde{C}_i + \frac{k_{DP}}{k_P}} = \frac{\tilde{C}_i}{\widetilde{C_\iota} + IC_{pSTAT}} \tag{S50}$$

where IC_{pSTAT} is the number of complexes per T-cell required for half-maximum STAT4 activation and is equivalent to $\frac{k_{DP}}{k_P}$.

IL-12 Receptor Dynamics

In the compartment where receptor binding occurs, we represent the concentration of receptor based on a basal production rate, an upregulated production rate based on STAT4 activation, consumption via binding, and unbound internalization/clearance. Accordingly, the differential equation describing the concentration of receptor is given by:

$$\frac{dR_i}{dt} = \frac{N_i}{V_i} k_R + \frac{N_i}{V_i}\, \alpha\, pSTAT_i - k_{on}\, IL12_i\, R_i - k_{CR} R_i \tag{S51}$$

where k_R is the basal production rate per T-cell in pmol cells^{-1} days^{-1}, k_{CR} is the unbound receptor internalization rate in days $^{-1}$, and α is the feedback parameter representing upregulated

receptor production by STAT4 activation in pmol cells^{-1} days^{-1}. Furthermore, we set the steady-state concentration of receptor according to the following relationship:

$$R_{SS} = \frac{R_0 N_i}{V_i} \tag{S52}$$

Here, R_{ss} is the steady-state/initial concentration of receptor in the absence of any IL-12 and R_0 is the basal number of IL-12 receptors per T-cell in the absence of IL-12 and STAT4 activation. To ensure that the concentration of receptor remains at this level at steady state, we constrain the basal production rate k_R according to:

$$k_R = R_0 k_{CR} \tag{S53}$$

IL-12 Clearance

In addition to receptor-mediated clearance, IL-12 can exit the body in our model via degradation in the subcutaneous space or traditional serum clearance. Clearance from the serum is determined by the first order clearance rate constant k_{CB} in days^{-1}. Instead of directly specifying the degradation rate of IL-12 in the subcutaneous space, we specify the absolute bioavailability (fraction of IL-12 in the subcutaneous space that does not get degraded) and determine the corresponding degradation rate. Accordingly, the degradation of IL-12 in the subcutaneous space is determined by:

$$k_{DG} = \frac{1 - F}{F} J_{xS} \tag{S54}$$

where k_{DG} is the first-order subcutaneous degradation rate constant and J_{xS} is the first-order transport rate constant from the subcutaneous space to compartment *x,* both in days^{-1}. In the accelerated-clearance model, this transport rate is that of IL-12 to the blood and in the reduced bioavailability model it is that of IL-12 to the lymphatic system.

Model of Intraperitoneal IL-12 Injection

We developed the reduced-bioavailability model to simulate subcutaneous dosing of IL-12; thus, we modified our model slightly to fit intraperitoneal injection data presented by Lenzi et al.[9]. All model equations here are identical to the original model equations (other than slight notation changes) except the equation determining the initial concentration of IL-12 in the intraperitoneal cavity. In the clinical trial data presented by Lenzi and colleagues, the initial concentration of IL-12 in the intraperitoneal cavity is two orders of magnitude lower than expected given the reported dose amount. To account for this, we add the scaling factor β to our expression for the initial concentration of IL-12 in the intraperitoneal cavity to obtain:

$$IL12_{P,0} = \beta \frac{D}{V_P} \tag{S55}$$

Here, β is a factor between zero and one that accounts for the discrepancy between the reported dose and initial concentrations of IL-12. Adding in this change and changes in notation to reflect IL-12 administration to the peritoneal cavity, we obtain equations S20-29

Model of Continuous, Local IL-12 Delivery

We further modified our model to represent continuous, local delivery of IL-12 within the intraperitoneal cavity. All equations in this model are identical to that of intraperitoneal injection of IL-12 except for the equations governing IL-12 in the intraperitoneal space. Here, the ordinary differential equation describing the concentration of IL-12 in the intraperitoneal space is now given by:

$$\frac{dIL12_P}{dt} = k_{pr}(t) - J_{LP}\, IL12_P - k_{DG}\, IL12_P \tag{S56}$$

Here, $k_{pr}(t)$ is the 0th-order production rate of IL-12 that varies with time according to the dosing strategy being simulated in pmol days^{-1}. We test three different dosing strategies

designed to reach equivalent i.p. concentrations at long times: 1) constant production, 2) stepwise production, and 3) linearly increasing production. These production profiles are given by:

$$k_{prod}(t) = \begin{cases} 0, & t < t_1 \\ k_{pr}^f, & t \geq t_1 \end{cases} \tag{S57}$$

$$k_{prod}(t) = \begin{cases} \frac{1}{3}k_{pr}^f, & t_1 \leq t \leq t_2 \\ \frac{1}{2}k_{pr}^f, & t_2 < t \leq t_3 \\ k_{pr}^f, & t > t_3 \end{cases} \tag{S58}$$

$$k_{prod}(t) = \begin{cases} 0, & t < t_1 \\ \frac{k_{pr}^f - k_{pr}^0}{t_2 - t_1}(t - t_1), & t_1 \leq t \leq t_2 \\ k_{prod}^f, & t > t_2 \end{cases} \tag{S59}$$

In the equations above k_{pr}^f is the final production rate reached by each production profile, and t_1 is the time dosing begins. The stepwise production profile is further characterized by t_2 and t_3, which are the times when IL-12 production is increased. Similarly, the linearly increasing production profile is characterized by t_1 and t_2, the time in which the increase in production rate begins and ends, respectively. All characteristic times of dosing profiles are given in days. Additionally, the initial production rate here is defined by k_{pr}^0.

<u>Parameter Optimization Error Functions</u>

The error functions used for optimization depend on the type of data and the number of compartments for which data was available. For time course data presented for a single compartment, we used a modified version of the sum of standard squared error to account for the assay's limit of detection:

$$SSE = \sum_i \begin{cases} (P_i - E_i)^2; P_i > D, E_i > D \\ (P_i - D)^2; P_i > D, E_i \leq D \\ 0; P_i \leq D, E_i \leq D \end{cases} \quad \text{(S60)}$$

where E_i is the value of experimental datapoint i, P_i is the model predicted value of that datapoint, and D is the lowest limit of detection for the quantification assay. For time course data where data is presented for more than one compartment, i.e., blood and intraperitoneal IL-12 measurements, the error function was further modified to normalize to the magnitude of the experimental measurement according to:

$$NSE = \sum_i \begin{cases} \frac{(P_i - E_i)^2}{E_i^2}; P_i > D, E_i > D \\ \frac{(P_i - D)^2}{D^2}; P_i > D, E_i \leq D \\ 0; P_i \leq D, E_i \leq D \end{cases} \quad \text{(S61)}$$

The error function used for optimizing to PK metric data is given by the following:

$$SSE = \sum_i \frac{(P_i - E_i)^2}{E_i^2 + \sigma_i^2} \quad \text{(S62)}$$

Here, E_i is the value of the PK metric measured in the clinical trial, σ_i is the reported standard deviation of the PK metric, and P_i is the model predicted value.

Local Model Sensitivity Analyses

Local sensitivity analyses were implemented to determine the impact of model parameters on the extent of IL-12 PK desensitization. For the simulation of multiple repeated doses of the same amount, we quantify the amount of desensitization predicted as the ratio of IL-12 serum AUC after the last and first dose according to:

$$\chi = \frac{AUC_{last}}{AUC_{first}} \quad \text{(S63)}$$

To determine the sensitivity of the quantity χ to a given parameter p, we calculated the log gain sensitivity according to:

$$S = \frac{\partial \ln(\chi)}{\partial \ln(p)} = \frac{\Delta \ln(\chi)}{\Delta \ln(p)} \quad \text{(S64)}$$

Ensemble Analysis of Desensitization Requirements

To expand on the influence of the parameters related to receptor lifetime, initial receptor concentrations, and feedback dynamics we generated an ensemble of 10,000 parameter sets varying $k_{CR}, k_{int}, N_{cells}, \alpha, R_0,$ and IC_{pSTAT} between 50% and 150% of the optimized values holding all other parameters constant. Each parameter set was simulated for two consecutive 1.0 μg/kg doses on days 1 and 8 of a 15-day cycle, and the amount of desensitization predicted was quantified based on equation 24. Analysis of these simulations illustrated that the amount of desensitization that occurs is correlated to the increase in binding flux at the time of the second dose (t = τ) normalized by the total flux of IL-12 out of the lymphatic system at the time of the first dose (t = 0), determined by equation 30. More specifically, we found that the value Ψ was inversely correlated to the AUC ratio and, therefore, positively correlated with the extent of desensitization predicted (**Supplemental Figure S7A**)

$$\Psi = \frac{R(\tau) - k_{on}R(0)}{J_{BL} + k_{on}R(0)} \quad \text{(S65)}$$

To gain deeper insight into the role specific parameters have on the amount of receptor remaining at the time of the second dose and the amount of desensitization predicted, we derived an analytical approximation for the concentration of receptor in the lymphatic system following a single dose (equations S74-78) This approximation of receptor concentrations is in reasonable agreement with numerical simulations, especially at longer time points where the receptor concentration is close to baseline levels (**Supplemental Figure S8**). Using this approximation to calculate the increase in receptor binding flux at the time of second dose based on equation S65, we obtain:

$$\Psi = \frac{k_{on}[e_1(\tau) + e_2(\tau) + e_3(\tau)]}{J_{BL} + k_{on}R(0)} \quad \text{(S66)}$$

Here, the three exponential terms $e_1(t), e_2(t)$, and $e_3(t)$ are given by equations S75-77. When used to predict the magnitude of IL-12 desensitization that occurs, equation S66 yields similar results to those extracted from numerical simulations (**Supplemental Figures S7B and S9**). Our analytical expression illustrates how specific parameters influence the amount of desensitization predicted without numerical simulation. We see that terms in the numerator of ϕ will lead to a larger peak in receptor concentration, and vice versa for the denominator. Additionally, increases in the three exponential decay parameters, $J_{LS}, k_{int},$ and k_{CR}, lead to faster receptor clearance. If all three decay timescales are sufficiently short, upregulated receptor will clear by the time of the second dose and desensitization will not be predicted. Furthermore, we predict that multiple processes in our model contribute to the presence of desensitization, and that desensitization will be predicted over a variety of different parameter combinations. Generally, the requirement for desensitization in our model is that the upregulated of IL-12 receptor remains present when the next dose is administered. We show here that this behavior is not specific to a small subset of parameter values, supporting the robustness of our model to predict desensitization despite the inherent variability in our model parameters.

<u>Derivation of Analytical Approximation for Receptor Dynamics</u>

To approximate the concentration of IL-12 receptor in the reduced-bioavailability model over time with an analytical expression, we aimed to approximate species in the model with exponential expressions. As the upregulation of receptor is regulated by the amount of STAT4 activation in T-cells, which is in turn regulated by the amount of IL-12:IL-12 receptor, we start by approximating the amount of complex formation that occurs in the lymphatic system. The

ordinary differential equation describing the concentration of complex formed is given in equation S13. Importantly, this differential equation is nonlinear due to the $k_{on}IL12_L R_L$ term. As a linear approximation, we assume that the binding flux is equal to the flux into the lymphatic system such that $k_{on}\ IL12_L\ R = \frac{J_{LS}V_S}{V_L}\ IL12_S$, giving us:

$$\frac{dC_L}{dt} = \frac{J_{LS}V_S}{V_L}\ IL12_S - k_{int}C_L \tag{S67}$$

The concentration of IL-12 in the subcutaneous space, $IL12_S$, is described by a single exponential decay since for this model we assume bioavailability (F) is one. The exponential decay describing the concentration of IL-12 in the subcutaneous space is given by:

$$IL12_S(t) = \frac{D}{V_S}\exp\{-J_{LS}t\} \tag{S68}$$

Making this substitution allows us to solve equation S67 analytically to obtain the dual exponential decay given by:

$$C_L(t) = \frac{J_{LS}D}{(k_{int} - J_{LS})V_L}[\exp\{-J_{LS}t\} - \exp\{-k_{int}t\}] \tag{S69}$$

Based on equations S15 and S16, we can now approximate the level of STAT4 activation according to:

$$pSTAT(t) = \frac{\frac{6.023e11V_L}{N_{cells}}C(t)}{\frac{6.023e11V_L}{N_{cells}}C(t) + IC_{pSTAT}} \tag{S70}$$

These approximations for the concentration of complex and STAT4 activation are in reasonable agreement with numerical simulations (**Supplemental Figure S10**). However, there is a slight overprediction of both species, likely due to our assumption that binding flux is equal to the total flux of IL-12 into the lymphatic system. To account for this difference, we rescale our approximation for the amount of complex formed by the initial ratio of binding flux to total flux, such that $C_L(t)$ is now given by:

$$C_L(t) = \frac{\frac{k_{on}R_0N_{cells}}{V_L}}{\frac{k_{on}R_0N_{cells}}{V_L} + J_{BL}} \frac{J_{LS}D}{(k_{int} - J_{LS})V_L} [\exp\{-J_{LS}t\} - \exp\{-k_{int}t\}] \quad \text{(S71)}$$

As seen in **Supplemental Figure S10** (blue curves), this slightly increases the accuracy of our analytical approximations compared to numerical simulations. Using equations S12 and S70, we can now solve for an analytical approximation for the concentration of receptor in the lymphatic system after linearizing the equation. Here, we make an important assumption that at long times (around the time of the next dose, which is our time span of interest), the amount of IL-12 in the lymphatic system is negligible such that $k_{on}IL12_LR \approx 0$. Additionally, our expression for $pSTAT(t)$ is non-linear; however, in the parameter regime we are operating $IC_{pSTAT} \gg \frac{6.023e11V_L}{N_{cells}} C_L(t)$, thus we can assume this function is approximately linear as given by:

$$pSTAT(t) = \frac{6.023e11V_L}{N_{cells}\, IC_{pSTAT}} C(t) \quad \text{(S72)}$$

Thus, our ordinary differential equation for receptor concentrations in the lymphatic system becomes linear, given by:

$$\frac{dR_L}{dt} = \frac{N_L}{V_L} k_R + \frac{N_L}{V_L}\, \alpha\, \frac{6.023e11V_L}{N_{cells}\, IC_{pSTAT}} C_L(t) - k_{CR}R_L \quad \text{(S73)}$$

This ordinary differential equation can be solved analytically and making the important substitution $k_R = k_{CR}R_0$, we obtain:

$$R(t) = \frac{R_0N_{cells}}{V_L} + e_1(t) + e_2(t) + e_3(t) \quad \text{(S74)}$$

$$e_1(t) = \frac{\Phi exp\,(-J_{LS}t)}{(J_{LS} - k_{int})(J_{LS} - k_{CR})} \quad \text{(S75)}$$

$$e_2(t) = \frac{\Phi \exp(-k_{int}t)}{(k_{int} - J_{LS})(k_{int} - k_{CR})} \tag{S76}$$

$$e_3(t) = \frac{\Phi \exp(-k_{CR}t)}{(k_{CR} - k_{int})(k_{CR} - J_{LS})} \tag{S77}$$

$$\Phi = \frac{6.023e11 J_{LS} \alpha D}{V_L IC_{pSTAT}} \frac{\frac{k_{on} R_0 N_{cells}}{V_L}}{\frac{k_{on} R_0 N_{cells}}{V_L} + J_{BL}} \tag{S78}$$

References

1. Motzer RJ, Rakhit A, Schwartz LH, et al. Phase I trial of subcutaneous recombinant human interleukin-12 in patients with advanced renal cell carcinoma. *Clinical Cancer Research*. 1998;4(5):1183-1191.

2. Rakhit A, Yeon MM, Ferrante J, et al. Down-regulation of the pharmacokinetic-pharmacodynamic response to interleukin-12 during long-term administration to patients with renal cell carcinoma and evaluation of the mechanism of this “adaptive response” in mice. *Clinical Pharmacology & Therapeutics*. 1999;65(6):615-629. doi:10.1016/S0009-9236(99)90083-8

3. Portielje JEA, Kruit WHJ, Schuler M, et al. Phase I Study of Subcutaneously Administered Recombinant Human Interleukin 12 in Patients with Advanced Renal Cell Cancer. *Clinical Cancer Research*. 1999;5(12):3983-3989.

4. Chizzonite R, Truitt T, Desai BB, et al. IL-12 receptor. I. Characterization of the receptor on phytohemagglutinin-activated human lymphoblasts. *The Journal of Immunology*. 1992;148(10):3117-3124. doi:10.4049/jimmunol.148.10.3117

5. Sender R, Weiss Y, Navon Y, et al. The total mass, number, and distribution of immune cells in the human body. *Proceedings of the National Academy of Sciences*. 2023;120(44):e2308511120. doi:10.1073/pnas.2308511120

6. Milewski M, Manser K, Nissley BP, Mitra A. Analysis of the absorption kinetics of macromolecules following intradermal and subcutaneous administration. *European Journal of Pharmaceutics and Biopharmaceutics*. 2015;89:134-144. doi:10.1016/j.ejpb.2014.11.013

7. Varkhede N, Forrest ML. Understanding the Monoclonal Antibody Disposition after Subcutaneous Administration using a Minimal Physiologically based Pharmacokinetic Model. *J Pharm Pharm Sci*. 2018;21(1 Suppl):130s-148s. doi:10.18433/jpps30028

8. Supersaxo A, Hein WR, Steffen H. Effect of Molecular Weight on the Lymphatic Absorption of Water-Soluble Compounds Following Subcutaneous Administration. *Pharm Res*. 1990;7(2):167-169. doi:10.1023/A:1015880819328

9. Lenzi R, Rosenblum M, Verschraegen C, et al. Phase I Study of Intraperitoneal Recombinant Human Interleukin 12 in Patients with Müllerian Carcinoma, Gastrointestinal Primary Malignancies, and Mesothelioma1. *Clinical Cancer Research*. 2002;8(12):3686-3695.